

OAK RIDGE NATIONAL LABORATORY LIBRARIES



3 4456 0550197 1

19.2

MICROINSTABILITIES IN  
INHOMOGENEOUS PLASMAS II:  
NUMERICAL RESULTS

C. O. Beasley, Jr.  
H. R. Hicks  
W. M. Farr  
J. E. McCune

OAK RIDGE NATIONAL LABORATORY  
CENTRAL RESEARCH LIBRARY  
DOCUMENT COLLECTION

**LIBRARY LOAN COPY**

DO NOT TRANSFER TO ANOTHER PERSON

If you wish someone else to see this  
document, send in name with document  
and the library will arrange a loan.

UCN-7969  
(3 3-67)



**OAK RIDGE NATIONAL LABORATORY**  
OPERATED BY UNION CARBIDE CORPORATION • FOR THE U.S. ATOMIC ENERGY COMMISSION

This report was prepared as an account of work sponsored by the United States Government. Neither the United States nor the United States Atomic Energy Commission, nor any of their employees, nor any of their contractors, subcontractors, or their employees, makes any warranty, express or implied, or assumes any legal liability or responsibility for the accuracy, completeness or usefulness of any information, apparatus, product or process disclosed, or represents that its use would not infringe privately owned rights.

Contract No. W-7405-eng-26

Thermonuclear Division

MICROINSTABILITIES IN INHOMOGENEOUS PLASMAS II:

NUMERICAL RESULTS

C. O. Beasley, Jr. and H. R. Hicks  
Oak Ridge National Laboratory, Oak Ridge, Tennessee

W. M. Farr  
University of Arizona, Tucson, Arizona

J. E. McCune  
Massachusetts Institute of Technology, Cambridge, Massachusetts

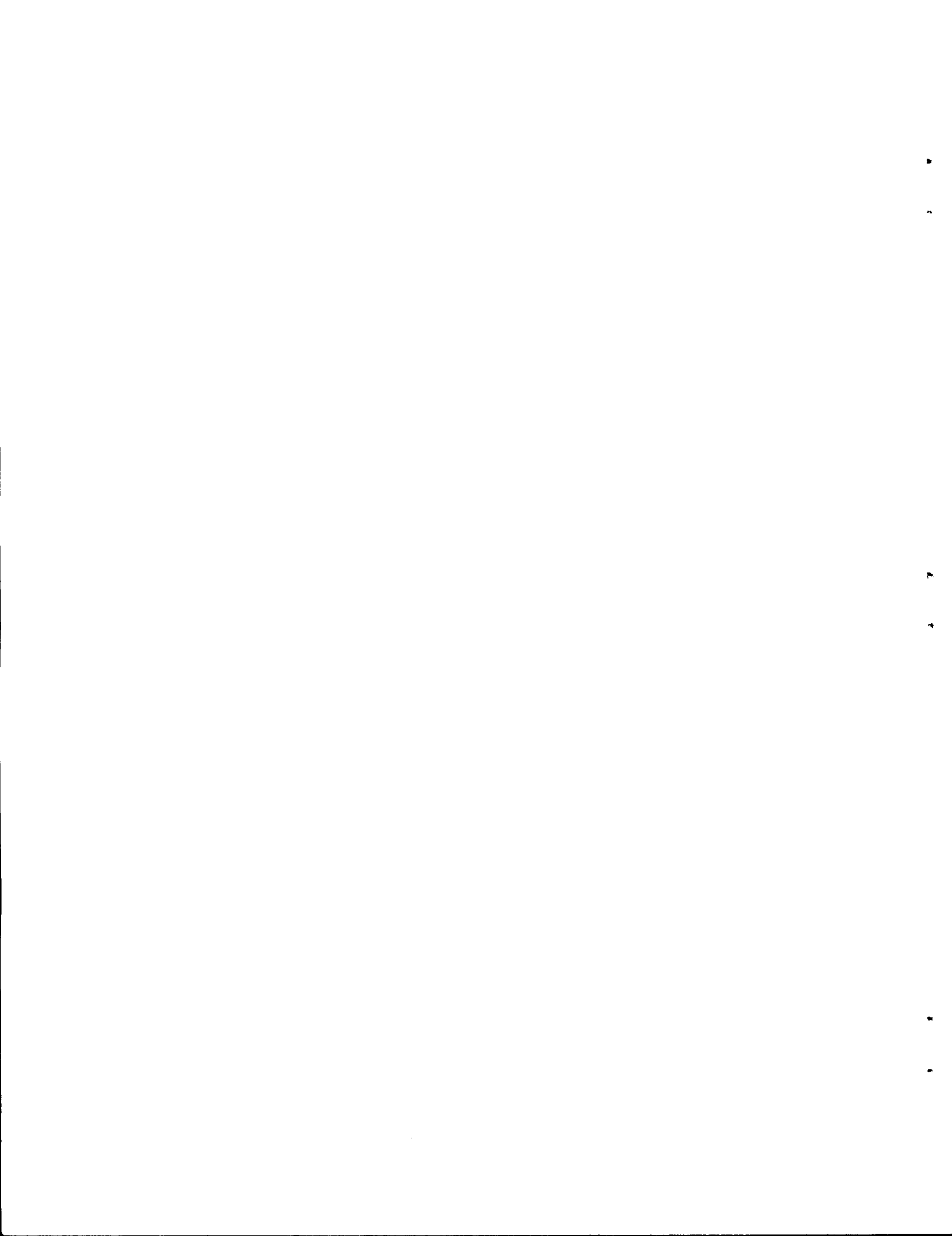
AUGUST 1973

OAK RIDGE NATIONAL LABORATORY  
Oak Ridge, Tennessee 37830  
operated by  
UNION CARBIDE CORPORATION  
for the  
U.S. ATOMIC ENERGY COMMISSION

OAK RIDGE NATIONAL LABORATORY LIBRARIES



3 4456 0550197 1



MICROINSTABILITIES IN INHOMOGENEOUS PLASMAS II:  
NUMERICAL RESULTS<sup>\*</sup>

C. O. Beasley, Jr. and H. R. Hicks  
Oak Ridge National Laboratory, Oak Ridge, Tennessee

W. M. Farr  
University of Arizona<sup>+</sup>, Tucson, Arizona

J. E. McCune  
Massachusetts Institute of Technology, Cambridge, Massachusetts

ABSTRACT

Results are presented from studies of microinstabilities in a model mirror plasma. The model has a Gaussian density distribution of ions and electrons along a varying magnetic field, and a radial density gradient perpendicular to this field. Particles are contained self-consistently by a fictitious confining potential modeling mirror confinement. The ion velocity-space distribution is the finite-plasma equivalent of a Guest-Dory loss-cone distribution, and the electron distribution allows for finite temperature effects, including Landau damping. Resonant and non-resonant loss-cone instabilities are discussed. It is found that resonant instabilities are stabilized when the plasma length is less than a critical length which is dependent upon electron temperature, but modes corresponding to flute modes in homogeneous plasmas (Dory-Guest-Harris and drift-cone) are found to remain unstable at all plasma lengths.

---

<sup>\*</sup>Research sponsored by the U.S. Atomic Energy Commission under contract with the Union Carbide Corporation.

<sup>+</sup>Work supported in part by National Science Foundation under Grant No. 5010-2222-18.

## I. INTRODUCTION

In an earlier paper,<sup>1</sup> hereafter referred to as (I), a formalism was developed for the investigation of microinstabilities in a model mirror plasma with a Gaussian density variation along the magnetic field [ $\vec{B} = \hat{z}B(z)$ ]. In (I), we used a model confining potential for both ions and electrons; we were able to solve the linearized Vlasov equation for the perturbed charge density. We then used Poisson's equations with appropriate boundary conditions to form an eigenvalue problem.

In the present paper, we first describe improvements in the model which allow for various physical effects not included in the earlier work. In the ions, we allow for lowest-order effects from a varying magnetic field<sup>2</sup>  $B(z) = B_0(1 + z^2/L_m^2)$ ; these result in a cyclotron frequency  $\Omega_i = \Omega_i(z)$ . A separable velocity-space distribution of the Guest-Dory form<sup>3</sup> [as also used in (I)] is used to include loss-cone, cyclotron damping, and ion thermal effects along the magnetic field. Ion bounce effects are not included, as seems to be justified when a magnetic-field variation exists.<sup>4</sup>

In the original model, electron bounce resonances resulting from the assumed parabolic confining potential for electrons result in regeneration effects which obviate electron Landau damping. To circumvent this, we have included in the theory a slight distortion of the parabolic confining potential. This distortion results in an energy-dependent bounce frequency, and therefore electron Landau damping. This model is described elsewhere,<sup>5</sup> and application to the present problem is described in this paper. The electron term also contains a radial density gradient to allow for the study of the drift-cone instability.<sup>6</sup>

In sufficiently short plasmas, modes corresponding to various distinct instability mechanisms do not appear as separate entities; rather we find only one unstable mode whose characteristics can be made up of a composite of several instabilities. Nevertheless, it is possible to pick certain combinations of the plasma parameters, such as density, shape of the perpendicular loss-cone, perpendicular density gradient, and electron temperature, for which one or the other instability mechanism clearly dominates, and for which, if the plasma length is allowed to become very long, one can recover the corresponding infinite-plasma mode. In this sense, we identify two different categories of modes studied: 1) those which in an infinite-length plasma occur with  $k_{\parallel} = 0$  (infinite wavelength along the magnetic field) and whose frequency is not resonant with the ion gyroharmonics (here are included the Dory-Guest-Harris<sup>7</sup> and drift-cone<sup>6</sup> instabilities); 2) the resonant loss-cone instabilities (here are included the absolute loss-cone instability<sup>8</sup> and the unstable negative-energy modes first studied by Berk et al<sup>9</sup>). In studying the behavior of these modes very near threshold, we find that as the confining potential of the electrons approaches a purely parabolic potential, we see a coupling of the unstable ion wave with stable electron plasma oscillations. We also study and discuss these threshold effects.

If we choose our ion distribution function so as to preclude the Dory-Guest-Harris mode, and if we eliminate the drift-cone mode by making the radial density gradient sufficiently small, we find at relatively short lengths a composite resonant instability which is a combination of

the absolute mode and the longest wavelength negative-energy mode. This unstable mode eventually stabilizes below some length  $L_p/a_i \approx 2 \sqrt{\frac{T_e M_i}{T_i m_e}}$ . This length is thus dependent on electron temperature. In previous work<sup>10</sup> this mode was studied in the absence of electron thermal effects.

While our numerical results are model dependent, they also show that for the purposes of calculating threshold densities and stabilizing lengths, such effects cannot be neglected.

By contrast, if the drift-cone, or Dory-Guest-Harris instability, or both are present, the residual mode cannot be stabilized by finite-length effects, as has been found previously.<sup>2, 11</sup> That is, no matter what the plasma length, the mode continues to appear in the plasma density range (corresponding to a line-averaged density) over which the infinite-plasma  $k_{\parallel} = 0$  mode can exist. Since the flute-like modes generally require much higher densities than the resonant modes, the threshold characteristics for this residual mode will vary widely as to both density and frequency depending on whether or not the plasma length permits the existence of a resonant mode. In other words, as the density is lowered, the mode characteristics become similar to those of the resonant mode if it can exist at that plasma length. Otherwise, the threshold density remains high corresponding to the absence of a resonant mode.

In section II of this paper, we discuss the formulation of the Fourier-analyzed perturbed charge density (the  $R_{\ell\mu}$  matrix in I). Part II A deals with the electron term, and part II B with the ion term. In section III we present and discuss results. We first discuss the resonant modes in the absence of Dory-Guest-Harris and drift-cone (flute-like) modes. Included in this discussion is the role of the electrons, including the part played by Landau damping. Finally we discuss the flute-like modes. In the final section (IV), we make some comments relevant to the impact of these results on the mirror confinement program in general, and future calculations in particular.

## II. THE NEW R-MATRIX

In generalizing the work reported in (I) we wish to incorporate a magnetic field variation, since in the absence of electron thermal effects, this, in combination with ion thermal effects, has been shown to be stabilizing to resonant instabilities. In addition, we wish to take account of radial as well as axial gradients in order to allow study of the drift-cone mode in addition to the resonant and non-resonant instabilities which do not depend on cross-field gradient effects. In general, this requires simultaneous treatment of both a radial as well as an axial eigenvalue problem. The situation is greatly simplified, however, by the fact that the radial part of the problem can be treated in the "local" approximation;<sup>12</sup> in this case the properties of the wave depend parametrically on conditions at each given flux surface, and on each such surface a purely axial eigenvalue problem can be defined.

In a spatially confined system the perturbation potential,  $\psi(z)$ , satisfies an integral equation. Alternatively, as explained in (I) we can form a matrix eigenvalue problem by Fourier analyzing  $\psi(z)$  over a length extending from the center of the machine to points on either side where the equilibrium density has fallen sufficiently so that  $k_{\perp} \lambda_{\text{Debye electron}} \gg 1$ . At these ends we require  $\psi = \psi'(z) = 0$ . Thus in this work the problem is actually treated in terms of a periodic system with the period sufficiently long so that each plasma "period" becomes a separate entity physically.

The contributions to the R-matrix can be derived by determining the electron and ion density perturbations using orbit-integral solutions to the Vlasov-equations. The results, for the electron and ion contributions

are detailed in the next two sections.

### A. The Electrons

The periodic "bounce" motion of the electrons in their confining potential  $\Phi(z)$  plays an important role in establishing the properties of the instabilities which can occur in mirror devices at realistic machine lengths and electron temperatures. In turn, the nature of this role depends crucially on the extent to which Landau damping occurs, that is to say, on the extent to which the bounce frequency is energy dependent. In any but an exactly parabolic potential well the energy dependence of the bounce frequency allows wave-particle resonance only for particles of specific discrete energies, and Landau damping appears. The case of an exactly parabolic well is degenerate:  $\omega_b = \text{constant}$  and no Landau damping occurs.<sup>13</sup>

Despite its degeneracy, it is frequently convenient to assume, as in (I), parabolic-well confinement, particularly in the description of the plasma equilibrium. The most important effect of departure from quadratic behavior of the confining potential is in the particle-wave resonances. For this reason we use a model of the electron dynamics, developed in reference 5, appropriate for "almost parabolic" confining potentials. A feature of this approach is that it allows us to retain the assumptions of parabolic well confinement except where treating particle-bounce resonance.

We assume an equilibrium distribution for the electrons of the form

$$\hat{f}_{oe}(E, v_{\perp}, x + \frac{v_y}{\Omega_e}) = \frac{1}{\pi^{3/2} \alpha^3} \exp\left(-\frac{2E}{\alpha^2} - \frac{v_{\perp}^2}{\alpha^2}\right) \left(1 + \epsilon\left(x + \frac{v_y}{\Omega_e}\right)\right) \quad (1)$$

$$\equiv f_o(E, v_{\perp}) \left(1 + \epsilon\left(x + \frac{v_y}{\Omega_e}\right)\right)$$

where

$$E = \frac{\Phi(z)}{m_e} + \frac{v^2}{2}$$

$$v_{\perp}^2 = v_x^2 + v_y^2 ;$$

$x$  is the local "radial" coordinate, measured from the flux surface of interest locally normal to  $y$  and  $z$ .

The distribution function  $\hat{f}_{oe}(\vec{v}, x)$  is normalized so that the equilibrium electron density along  $\vec{B}$  is

$$\begin{aligned} n_o(z, x) &= n_o(o, o) \int d^3\vec{v} \hat{f}_o(E, v_{\perp}, x + \frac{v_y}{\Omega_e}) \\ &= n_o(o, o) (1 + \epsilon x) \int dv F_o(E) \end{aligned}$$

where  $F_o(E) = \int d^2v_{\perp} f_o(E, v_{\perp})$ . (This formula is intended to hold only locally around the flux surface  $x = 0$ , generally taken to be at the position of maximum radial density gradient.)

Correspondingly the electron density perturbation is obtained from the perturbation of the electron distribution function:

$$n(z, t, k_y) = n(o, o) \int d^3\vec{v} f_e(\vec{v}, k_y, z, t)$$

We introduce the Fourier analysis of the perturbation potential appropriate to the local approximation:

$$\psi(y, z, t) = \exp(ik_y y) \hat{\psi}(k_y, z, t)$$

$$\hat{\psi}(k_y, z, t) = \sum_{\mu=-\infty}^{\infty} \varphi_{\mu}(t) \exp(i\mu z/L_p)$$

(2)

where  $L_p = \alpha/\omega_{bo}$  is the plasma length and  $\omega_{bo}$  is the bounce frequency for thermal particles ( $\omega_0(E)$  at  $E = \alpha^2/2$ ). Then the solution to the linearized Vlasov equation obtained from the standard orbit integral can be written

$$f_e(\vec{v}, k_y, z, t) = \frac{q_e}{m_e} \sum_{\mu} \int_0^t dt' \left[ \frac{\partial \hat{f}_{oe}}{\partial E} i\mu \frac{v'}{L_p} + \frac{ik_y v'_y}{v_{\perp}} \frac{\partial \hat{f}_{oe}}{\partial v_{\perp}} + \frac{ik_y \epsilon}{\Omega_e} f_o \right] \times \\ \times \exp[ik_y(y'-y)] \times \exp[i\mu z'/L_p] \varphi_{\mu}(t') \quad (3)$$

where the primed quantities are orbit variables satisfying, for example,

$$\frac{dz'}{dt'} = v'(v, z, t'-t); \quad \frac{dv'}{dt'} = \frac{1}{m_e} \frac{d\Phi}{dz'} \quad (4)$$

with the "initial" conditions

$$v'(t'=t) = v, \quad z'(t'=t) = z$$

In Eq.(3) we have neglected the contribution to  $f_e$  at  $t = 0$  since we are interested in growing solutions (instabilities).

We now assume  $k_{\perp} a_e = k_{\perp} \frac{\alpha}{\Omega_e} \ll 1$ . In this limit the Larmor motion is unimportant and we may put  $\exp[ik_y(y'-y)] = 1$ . Then, upon integration over  $\vec{v}_{\perp}$ , the terms in  $v_y$  average to zero. This small Larmor radius limit could, of course, also be obtained directly from the drift kinetic equation.

Integrating over  $\vec{v}$  in (3) and taking the Laplace transform then yields (at  $x = 0$ )

$$\frac{q_e n_e}{\epsilon_0} (k_y, z, \omega) = \omega_{pe}^2 \sum_{\mu} \varphi_{\mu}(\omega) \int_{-\infty}^{\infty} dv \int_{-\infty}^0 d\tau \exp(-i\omega\tau) \left[ i\mu \frac{v'(\tau)}{L_p} \frac{\partial F_o}{\partial E} + i \frac{k_y \epsilon}{\Omega_e} F_o \right] \times \\ \times \exp(i\mu z'/L_p) \quad (5)$$

where  $\omega_{pe}^2$  is the plasma frequency at  $z = 0$ , and  $F_0(E) = \int d^2 \vec{v}_\perp f_0(E, v_\perp)$ .

We may Fourier analyze this result in the form

$$n_e(k_y, z, \omega) = \sum_l N_l \exp(i l z / L_p)$$

$$N_l = \frac{1}{2\pi L_p} \int_{-\pi L_p}^{\pi L_p} dz n_e(z) \exp(-i l z / L_p) \quad (6)$$

yielding

$$\frac{q_e N_l}{\epsilon_0} = \omega_{pe}^2 \sum_\mu \int_{-\infty}^{\infty} dv \int_{-\pi L_p}^{\pi L_p} \frac{dz}{2\pi L_p} \int_{-\infty}^{\infty} d\tau \exp(i\omega\tau) \left[ i\mu \frac{v'(\tau)}{L_p} \frac{\partial F_0}{\partial E} + \frac{ik_y \epsilon}{\Omega_e} F_0 \right] \times$$

$$\times \exp(i\mu z' / L_p - ilz / L_p) \quad (7)$$

This result, when substituted into the Fourier expansion of Poisson's equation yields the electron contribution to the R-matrix. Further reduction of (7) requires knowledge of the parallel (bouncing) motion of the electrons and hence specification of  $\Phi(z)$ .

A method was developed in ref. 5 for treating the dynamics of particles confined in nearly parabolic potentials. We introduce the orbit phase angle  $\theta(\tau)$  through

$$\sqrt{\frac{\Phi(z')}{m}} = \sqrt{E} \cos \theta(\tau) ; \quad \frac{v'}{\sqrt{2}} = \sqrt{E} \sin \theta(\tau) \quad (8)$$

and note that

$$\frac{d\theta}{d\tau} = -\sqrt{2} \frac{d}{dz'} \sqrt{\frac{\Phi(z')}{m}} \quad (9)$$

We restrict our attention to potentials  $\Phi(z')$  which are symmetric about

$z' = 0$  and have only a single minimum. For such cases  $z'$  is a periodic function of  $\theta$  and hence of  $\tau$ . If  $\Phi(z')$  were purely parabolic,  $\Phi/m = \omega_{b0} z'^2/2$ , we would have simply

$$z' = \frac{\sqrt{2E}}{\omega_{b0}} \cos\theta, \quad \frac{d\theta}{d\tau} = -\omega_{b0}$$

For nearly periodic potentials we write

$$z' = \frac{\sqrt{2E}}{\omega_{b0}} \left( \cos\theta - 2 \sum_{n=0}^{\infty} B_{2n+1} \cos(2n+1)\theta \right) \quad (10)$$

where the coefficients  $B_n$  are functions of  $E$  alone and can be determined for specified  $\Phi(z')$  by the method of ref. 5. The  $B_n$ 's are very small for nearly parabolic potentials.

It is shown in ref. 5 that

$$\tau_b(E) \equiv \frac{2\pi}{\omega_b(E)} = \frac{2\pi}{\omega_{b0}} \left( 1 - 2 \sum_{n=0}^{\infty} (2n+1) B_{2n+1}(E) \right) \quad (11)$$

whereas

$$\frac{d\tau}{d\theta} = -\frac{1}{\omega_b(E)} \left( 1 - \sum_{m=1}^{\infty} a_m \cos 2m\theta \right) \quad (12)$$

with

$$a_m(E) = \frac{\omega_b(E)}{\omega_{b0}} \sum_{n=m}^{\infty} 4 (2n+1) B_{2n+1}$$

Then

$$-\omega_b(E) (\tau - \tau_0) = \theta - \frac{\pi}{2} - \sum_{m=1}^{\infty} \frac{a_m}{2m} \sin 2m\theta \quad (13)$$

where  $\tau_0$  is the value of  $\tau$  at  $\theta = \pi/2$ , where  $z' = 0$ .

In the orbit integral (8) we must distinguish between

$$z'(z, v, \tau) = \hat{z}(E, \tau - \tau_0)$$

and

$$z'(z, v, 0) = z = \hat{z}(E, -\tau_0);$$

Then, consistent with the periodicity of  $z'$  and  $z$  with respect to  $\tau$  and  $\tau_0$ , we write

$$\left. \begin{aligned} \exp(i\mu z'/L_p) &= \sum_{m=-\infty}^{\infty} S_m(E, \mu) \exp[im\omega_b(E)(\tau - \tau_0)] \\ \exp(i\ell z/L_p) &= \sum_{m=-\infty}^{\infty} S_m(E, \ell) \exp[im\omega_b(-\tau_0)] \end{aligned} \right\} \quad (14)$$

Note that the coefficients  $S_m$  are independent of the phase angles:

$$\begin{aligned} S_m(E, \mu) &= \frac{i}{\tau_b} \int_0^{\tau_b} d(\tau - \tau_0) \exp[-im\omega_b(\tau - \tau_0) + i\mu z'/L_p] \\ &= \frac{1}{2\pi} \int_{-\pi/2}^{5\pi/2} d\theta \left( 1 - \sum_{p=1}^{\infty} a_p \cos 2p\theta \right) \exp\{-im[\theta + \frac{\pi}{2} - \sum_{q=1}^{\infty} \frac{a_q}{2} \sin 2q\theta]\} \\ &\quad \times \exp\left\{i \frac{\mu}{L_p} \sqrt{2E/\omega_{b0}} \left( \cos\theta - 2 \sum_{n=0}^{\infty} B_{2n+1} \cos(2n+1)\theta \right)\right\} \end{aligned} \quad (15)$$

where we have used eqns. (10), (11), (14).

The integral in (7) involves integration over  $v$  and  $z$ . But we can replace these integrations by integrals over  $E$  and  $\tau_0$ , using

$$dv dz = dE d\tau_0 \quad (16)$$

since the Jacobian of the transformation from  $(z, v)$  to  $(E, \tau_0)$  is unity from Eqn.(8). Then, with the help of (14) the orbit integral in (7) can be written

$$\begin{aligned} \frac{qN_\ell}{\epsilon_0} &= \omega_{pe}^2 \sum_{\mu} \frac{\varphi_{\mu}}{L_p} \int_0^{\infty} dE \int_{-\infty}^0 d\tau \sum_{m=-\infty}^{\infty} S_m(E, \mu) S_m^*(E, \ell) \left[ im \frac{\partial F_0}{\partial E} + \frac{ik_y \epsilon}{\Omega_e \omega_b} F_0 \right] \times \\ &\quad \times \exp[-i(\omega - m\omega_b)\tau] \\ &= \frac{\omega_{pe}^2}{L_p} \left( \frac{-2}{\alpha^2} \right) \frac{1}{\sqrt{\pi\alpha}} \int_0^{\infty} \frac{dE}{\omega_b(E)} \sum_{\mu, m=-\infty}^{\infty} \varphi_{\mu} \frac{S_m(E, \mu) S_m^*(E, \ell)}{m\omega_b(E) - \omega} \exp(-2E/\alpha^2) [m\omega_b - \omega_*^e] \quad (17) \end{aligned}$$

where  $\omega_*^e = \epsilon k_y \alpha^2 / 2\Omega_e$ .

The integral over  $\tau$  in (17) is defined in the sense of a Laplace transform,  $\text{Im}(\omega) > 0$ , and the singular denominators in the subsequent energy integral are to be understood in this light. The behavior of the energy integral is crucially dependent on the behavior of  $\omega_b$  as a function of  $E$ . Indeed, if  $\omega_b = \omega_{b0} = \text{const.}$ , the integral does not exist for  $\omega = m\omega_{b0}$ . By contrast, if  $\omega_b = \omega_b(E)$  the resonances at the particular energies for which  $\omega = m\omega_b(E)$  simply contribute a finite imaginary part to the integral over  $E$ , as in classical Landau damping.

On the other hand, the departure from parabolic-well behavior of the quantities appearing in the  $S_m(E, \mu)$  is not so essential and useful approximations to the  $S_m$  can be obtained when  $\Phi(z)$  is almost parabolic. In particular, suppose that we can neglect the terms involving  $a_m$  and  $B_m$  in (15). Then

$$S_m(E, \mu) \cong \frac{1}{2\pi} \int_{-\pi/2}^{5\pi/2} d\theta \exp[-im(\theta + \pi/2) + i\mu \frac{\sqrt{2E}}{\alpha}] = J_m(\mu x) \quad (18)$$

where  $J_m$  is the Bessel function, and we have introduced the dimensionless energy variable  $x^2 = 2E/\alpha^2$ .

In what follows we assume that the departure from quadratic well confinement is slight enough that we can adopt the approximation (18) for the  $S_m$ 's, but we keep the essential energy dependence of  $\omega_p$ . Then,

$$\frac{qN_\ell}{\epsilon_0} = \frac{\omega_{pi}^2}{\sqrt{\pi} \alpha_{zi}^2} \sum_{\mu} \varphi_{\mu} R_{\ell\mu}^e \quad (19)$$

with

$$R_{\ell\mu}^e = \frac{T_{zi}}{T_e} \int_0^{\infty} 2x \, dx \exp(-x^2) \sum_{m=-\infty}^{\infty} \frac{J_m(\mu x) J_m(\ell x)}{\omega - m\omega_b(x)} \left[ m\omega_b(x) - \omega_*^e \right] \frac{\omega_{bo}}{\omega_b(x)} \quad (20)$$

where the ion-electron temperature ratio  $T_{zi}/T_e$  appears because of the normalization of the R-matrix with respect to the ion plasma density  $\omega_{pi}^2$ , and the ion parallel thermal speed  $\alpha_{zi}$ . When  $\omega_b(x) = \omega_{bo} = \text{const.}$  and  $\omega_*^e = 0$ ,  $R_{\ell\mu}^e$  reduces to the electron contribution to the R-matrix used in (I), in the small Larmor radius limit  $\lambda_e \rightarrow 0$ . When  $\omega_b = \omega_b(x)$ , however, the x-integral must be carried out numerically in general, and depends crucially on  $\omega_b(x)$ .

As a model of almost parabolic-well confinement we consider a confining potential of the form

$$\left. \begin{aligned} \frac{\Phi}{m} &= 0 \quad ; \quad |z| < z_0 \\ \frac{\Phi}{m} &= \frac{1}{2} \omega_{bo}^2 (|z| - z_0)^2 \left(1 + \frac{|z|}{L}\right)^2 \quad ; \quad |z| > z_0 \end{aligned} \right\} \quad (21)$$

When  $z_0 \ll L_p$ , and  $L \gg L_p$  this potential is almost parabolic in the sense that particles with thermal energy will experience very nearly a quadratic potential.

The bounce frequency associated with(21) has the form

$$\left. \begin{aligned} \frac{\omega_b(x)}{\omega_{b0}} &= \frac{x(1+ax)}{x+b} \\ a &= \frac{4}{\pi} \frac{L_p}{L}, \quad b = \frac{2}{\pi} \frac{z_0}{L_p} \end{aligned} \right\} \quad (22)$$

Note that  $\omega_b(x) = \omega_{b0}$  when  $x = \sqrt{b/a}$  so that if we choose  $b = a$  as in our actual computations, thermal particles will experience a bounce frequency equal to  $\omega_{b0}$ . When  $a$  and  $b$  are both very small,  $\omega_b(x)$  is very like a step function, increasing very rapidly to  $\omega_{b0}$  for small  $x$  and increasing only very slowly thereafter.

The quantities  $a$  and  $b$  are given above directly in terms of the shape of the model confining potential; an alternative interpretation of  $a$  is that it represents the fractional departure from quadratic-well confinement experienced by a thermal particle.

In ref. 5, practical means of computing the  $x$ -integral in  $R_{l\mu}^e$  both directly and approximately are discussed. In the following we restrict ourselves to a discussion of only the salient features.

As  $\omega$  approaches real values,  $\text{Im}(\omega) \rightarrow 0^+$ , imaginary contributions to the  $x$ -integral will arise from the residues at the points at which  $m\omega_b(x) = \omega$ . These contributions lead to Landau damping. It is clear from the form of the integrals in (20) that the maximum Landau damping from the  $m$ -th term in the sum occurs when  $\omega = m\omega_{b0}$ . For resonant, non-flute-like instabilities, for which Landau damping is most important,  $\omega$  will be near  $\Omega_1(z=0)$ . Thus, for short machines, at reasonable electron temperature,  $\omega = (m_0 \pm \delta)\omega_{b0}$  where  $m_0$  is less than 10, and  $0 \leq \delta \leq 1/2$ . With  $m_0$  in this range, maximum Landau damping occurs for  $\delta = 0$ ,  $\omega = m_0\omega_{b0}$ , and comes from the resonance at  $x = 1$  in the  $m_0$ -th integral in (20). For each

$m \neq m_0$  in the sum in (20) the resonances occur either at small  $x$  ( $|m| > |m_0|$ ) or large  $x$  ( $|m| < |m_0|$ ) and these contributions to the imaginary part of  $R_{\mu}^e$  are relatively small. Similarly when  $\omega$  is halfway between two moderate harmonics of  $\omega_{b0}$  ( $\delta = 1/2$ ) Landau damping will be small for all terms in the sum.

For long plasma lengths,  $\omega_{b0} \rightarrow 0$  and  $m_0$  becomes very large. In this case  $\omega/m\omega_{b0}$  will be near unity for a large number of the integrals in the sum in (20) and all of these will contribute approximately equal amounts of Landau damping. Eventually, as  $L_p \rightarrow \infty$ ,  $\omega_{b0} \rightarrow 0$ , the bounce structure is lost altogether and the infinite medium dispersion relation is recovered from (20) in a manner discussed by Baldwin and Rowlands.<sup>14</sup>

### B. Derivation of the Ion Contribution

The response of the ion density<sup>2</sup> is

$$\frac{qn_i}{\epsilon_0}(s) = - \frac{2\sqrt{\pi} i \omega_{pi0}^2 \omega L_p}{\alpha_1^2} \sum_n D_n^j \int_0^\infty \frac{dv_{\parallel}}{v_{\parallel}} f_{\parallel}(v_{\parallel}) \int_{-\infty}^\infty ds' n\left(\frac{s+s'}{2}\right) \hat{\psi}(s') \times$$

$$\times \exp\left[-i \int_t^{t'} dt'' (\omega - n\Omega_i(t''))\right] \theta(t' - t) \quad (23)$$

where  $D_n^j$  is the function given by Guest and Dory,<sup>3</sup> and where we have included only the loss-cone term in the ions ( $T = T_{\parallel}/T_{\perp} = 1$ ).

In the special case of a homogeneous magnetic field the variables  $s$  and  $s'$  would represent distances along a field line. Using

$$\sum_{\ell} R_{\mu\ell} \varphi_{\ell} = \frac{1}{2\pi L_p} \int_{-\infty}^{\infty} ds \exp(-ik_{\mu}s) 4\pi \rho_i(s) \quad (24)$$

and

$$\hat{\psi}(s') = \sum_{\ell} \varphi_{\ell} \exp(ik_{\ell}s') \quad (25)$$

we get

$$R_{\mu\ell} = \frac{-i \omega_{pi0}^2}{\sqrt{\pi} \alpha_1^2} \sum_n R_{\mu\ell}^{(n)} \quad (26)$$

where

$$R_{\mu\ell}^{(n)} = D_n^j \omega \int_{-\infty}^{\infty} ds \exp(-ik_{\mu}s) \int_{-\infty}^{\infty} ds' \exp(ik_{\ell}s') n\left(\frac{s+s'}{2}\right) \times$$

$$\times \int_0^\infty \frac{dv_{\parallel}}{v_{\parallel}} \exp\left[-i \int_t^{t'} dt'' (\omega - n\Omega_i(t''))\right] \theta(t' - t) f_{\parallel}(v_{\parallel}) . \quad (27)$$

Substituting  $dt'' = \pm ds/|v_{\parallel}|$  and using  $v_{\parallel}$  as a constant, and substituting  $\Omega_i(s) = \Omega_{i0}(1 + s^2/L_m^2)$ , we obtain

$$-i \int_t^{t'} dt'' \left( \omega - n\Omega_i(t'') \right) \theta(t' - t) = \frac{i}{v_{\parallel}} |s - s'| \left[ \omega - n\Omega_{i0} \left( 1 + \frac{(s+s')^2}{4L_m^2} + \frac{(s-s')^2}{12L_m^2} \right) \right]. \quad (28)$$

Making the change of variables to  $R = (s+s')/2$  and  $z = s - s'$  we obtain

$$R_{\mu\ell}^{(n)} = D_n^j \omega \int_{-\infty}^{\infty} dR \int_{-\infty}^{\infty} dz n(R) \int_0^{\infty} \frac{dv_{\parallel}}{v_{\parallel}} f_{\parallel}(v_{\parallel}) \quad (29)$$

$$\times \exp \left[ -i(k_{\mu} - k_{\ell}) R - i(k_{\mu} + k_{\ell}) z/2 + i \frac{|z|}{v_{\parallel}} \left( \omega - n\Omega_{i0} \left( 1 + \frac{(R^2 + z^2/12)/L_m^2}{L_m^2} \right) \right) \right].$$

Using  $n(R) = \frac{\exp(-R^2/L_p^2)}{\sqrt{\pi} L_p}$  the R integral can be done giving

$$R_{\mu\ell}^{(n)} = D_n^j \omega \int_{-\infty}^{\infty} dz \int_0^{\infty} \frac{dv_{\parallel}}{v_{\parallel}} \frac{f_{\parallel}(v_{\parallel})}{\sqrt{1 + \frac{\text{in}\Omega_{i0} |z| L_p^2}{v_{\parallel} L_m^2}}} \quad (30)$$

$$\times \exp \left[ -\frac{i}{2} (k_{\mu} + k_{\ell}) z + i \frac{|z|}{v_{\parallel}} (\omega - n\Omega_{i0}) - \frac{\text{in}\Omega_{i0} |z|^3}{12 L_m^2 v_{\parallel}} - \frac{L_p^2 (k_{\mu} - k_{\ell})^2}{4 \left( 1 + \frac{\text{in}\Omega_{i0} |z| L_p^2}{v_{\parallel} L_m^2} \right)} \right].$$

Letting  $\delta\omega = \omega - n\Omega_{i0}$  and  $f_{\parallel}(v_{\parallel}) = \frac{\exp(-v_{\parallel}^2/\alpha_{\parallel}^2)}{\sqrt{\pi} \alpha_{\parallel}}$  and making a change of variable from

z to  $\xi = n\Omega_{i0} z/v_{\parallel}$  one obtains

$$R_{\mu\ell}^{(n)} = - \frac{\omega D_n^j}{\Omega_{i0} \sqrt{\pi} \alpha_{\parallel n}} \int_{-\infty}^{\infty} d\xi \times$$

$$\times \int_0^{\infty} dv_{\parallel} \frac{\exp\left[-\frac{v_{\parallel}^2}{\alpha_{\parallel}} - i(k_{\mu} + k_{\ell}) \frac{v_{\parallel} \xi}{2n\Omega_{i0}} + \frac{i\delta\omega|\xi|}{n\Omega_{i0}} - \frac{iv_{\parallel}^2 |\xi|^3}{12L_m^2 n^2 \Omega_{i0}^2} - \frac{\frac{1}{4} L_p^2 (k_{\mu} - k_{\ell})^2}{1+i|\xi| L_p^2/L_m^2}\right]}{\sqrt{1+i|\xi| L_p^2/L_m^2}} \quad (31)$$

The  $v_{\parallel}$  integral can now be done giving

$$R_{\mu\ell}^{(n)} = \frac{\hat{\omega} D_n^j}{n} \int_0^{\infty} d\xi \frac{\exp\left[\frac{i\delta\hat{\omega}|\xi|}{n} - \frac{\frac{1}{4}(\mu-\ell)^2}{1+i|\xi| L_p^2/L_m^2} - \frac{\frac{1}{16}(\mu+\ell)^2 \xi^2 \hat{\omega}_{bi}^2}{n^2}\right]}{\sqrt{1+i|\xi| L_p^2/L_m^2} \sqrt{1+\frac{i|\xi|^3 \hat{\omega}_{bi}^2 L_p^2}{12 n^2 L_m^2}}} \quad (32)$$

where  $\delta\hat{\omega} \equiv \delta\omega/\Omega_{i0}$ ,  $\hat{\omega}_{bi} \equiv \omega_{bi}/\Omega_{i0}$ ,  $\hat{\omega} = \omega/\Omega_{i0}$ ,  $\mu = k_{\mu} L_p$ ,  $\ell = k_{\ell} L_p$  and we have let  $\alpha_{\parallel} = \omega_{bi} L_p$ . The absolute value of  $\xi$  can be replaced by  $\xi$  everywhere and the resulting integral can be done numerically by choosing appropriate paths in the complex  $\xi$ -plane.

## III. PRESENTATION OF RESULTS

In presenting our results, we first remark that we have restricted our findings to even modes, that is, modes for which  $\hat{\psi}(z) = \hat{\psi}(-z)$ . This class of modes allows us to study both the flute mode and modes with non-zero  $k_{\parallel}$ . It includes the instability of most interest, the one which remains unstable at the shortest plasma length. While it eliminates the longest-wavelength odd-parity mode, the characteristics of that mode are essentially the same as other finite- $k_{\parallel}$  modes which are studied.

Our primary concern is the investigation of loss-cone instabilities. We may divide these into two groups: resonant modes, and non-resonant (flute-like) modes. The non-resonant modes generally occur at densities  $\omega_{pi}^2/\Omega_i^2 \gtrsim 100$ , and involve ion-ion interactions (Dory-Guest-Harris instability<sup>7</sup>) or an interaction of the ion wave with the electron drift wave (drift-cone instability<sup>6</sup>). The resonant modes, on the other hand, involve either the destabilization of a negative-energy ion wave by dissipation associated with the flow of waves outwards to the ends of the system,<sup>9</sup> or else, in the case of the absolute instability, an interaction of an ion wave (with inverse cyclotron damping) with an electron wave-particle resonance.<sup>8</sup> One might expect the Dory-Guest-Harris instability to be insensitive to electron thermal effects. This should also be true for the flute-like drift-cone instability, since the perturbed charge density of the electrons for  $k_{\parallel} = 0$  is dominated by the electron drift term and is therefore independent of electron temperature. In contrast, the only contributions to the perturbed electron charge density in the case of resonant modes comes from  $k_{\parallel} \neq 0$  terms, and we might expect these modes to depend on electron temperature. In fact, we find that electron

thermal effects dominate the behavior of the resonant modes in short plasmas. This is discussed in the latter part of the section on resonant instabilities.

#### A. Resonant Instabilities

We will discuss results for unstable modes associated with the first gyro-harmonic, that is,  $\omega \sim \Omega_i$ . We have found that modes at higher gyro-harmonics stabilize at longer plasma lengths than those at the first harmonic, and are therefore not as critical. We will also restrict our numerical calculations to a single value of  $k_{\perp} a_i = 2.45$ . This value provides a reasonable approximation to the 'worst' case, that is the value which yields the highest growth rate instability at a given density over most of the range of plasma parameters investigated. Variations in this value will at most yield small quantitative differences in numerical results.

We first consider our results in the limit of long plasmas in order to connect with known results in that regime, and to better understand the connection between the two categories of results. To do this, we must first define what is meant by 'long plasma'. Two criteria must be satisfied:

1) The straight-line orbit approximation must be valid for all plasma species, and

2) the mode wavelength along the magnetic field must be much less than the plasma scale length.

We may use the straight-line orbit approximation if either  $\gamma \gg \omega_{be}$  or if  $\omega \Delta\tau \gg \pi$ ,<sup>4</sup> where  $\omega \sim \Omega_i$  and  $\Delta\tau$  is the thermal spread in the electron bounce period:  $\Delta\tau = \frac{1}{\omega_{be}} \left( \frac{\Delta \omega_{be}}{\omega_{be}} \right)$ . From our model of the electron bounce

motion, if we use a thermal width to define  $\Delta\omega_{be}$ , we find

$$\frac{\Delta\omega_{be}}{\omega_{be}} \approx 3/2 (a + b)$$

So

$$\omega_{be}/\Omega_i \ll \text{Max} \left( \gamma, \frac{a + b}{2} \right) \quad (33)$$

satisfies the criteria for use of the straight-line orbit approximation.

From equation (21),(I), we may write the R-matrix in this limit

$$R_{\ell\mu} = \left\{ \sum_n \left[ -\frac{nT}{\mu\hat{\omega}_{bi}} D_n^j(\lambda) Z \left( \frac{\hat{\omega}-n}{\mu\hat{\omega}_{bi}} \right) \right] + \frac{T_i}{T_e} \frac{1}{2} Z' \left( \frac{\hat{\omega}}{\mu\omega_{be}} \right) \right\} \exp [-(\ell-\mu)^2/4]$$

where we have included only the loss-cone term in the ions. (We have neglected the finite Larmor radius correction for the electrons and have corrected a sign error in the  $\exp[-(\ell-\mu)^2/4]$  term.) In order to obtain the long-plasma limit, we further assume that the  $\phi_\mu$  are large only in the neighborhood of a  $\mu \approx L_p/\lambda_{\parallel}$  such that  $\mu\omega_{be} \ll \omega \sim \Omega_i$ . Then we may write the electron term as

$$\frac{m_i}{2m_e} \frac{\mu^2 \hat{\omega}_{bi}^2}{\hat{\omega}^2} \exp [-(\ell-\mu)^2/4]$$

and it follows from the conditions above that

$$2\pi \hat{\omega}_{be} \ll \lambda_{\parallel}/L_p \ll 1$$

If we further assume a 'local' approximation for the ion term and at the same time take the asymptotic limit for the plasma dispersion function in the ion term, we may transform Poisson's equation back to configuration space and obtain

$$k_1^2 \psi(z) = \omega_{pe}^2(z/L_p) \left[ \frac{m_e}{M_i} \frac{1}{\alpha_1 z} \sum_n \frac{n D_n^i(\lambda)}{\omega - n} + \frac{1}{\omega} \frac{d^2}{dz^2} \right] \hat{\psi}(z) \quad (34)$$

If we now consider this equation in the vicinity of the origin and expand the density as  $\omega_{pe}^2(z) \approx \omega_{po}^2 (1 - z^2/L_p)$ , we at once recover the results of Berk, et. al.<sup>9</sup>

In(I) we noted that the infinite, homogeneous-plasma results did obtain from our formalism; (this also follows from equation (34) above). Since any mode we find will be a standing wave with zero group velocity, we would expect to be able to recover the absolute loss-cone instability<sup>8</sup> as well as the negative-energy modes discovered by Berk, et. al.<sup>9</sup>

We note in Fig. 1 the behavior of the negative-energy modes and the absolute instability as the magnetic field scale length is decreased. In obtaining these results, we have used the straight-line orbit approximation for electrons, neglecting bounce effects which at most would superimpose a small modulation on the curves in our model. Here we are considering modes with small growth rates, so the behavior is similar to threshold behavior. We have chosen  $j = T = 5$  so as to emphasize the loss-cone without introducing anisotropy effects. To simplify numerical calculation, we used (in these particular results only) a bi-Lorentzian velocity-space distribution for the ions instead of a Maxwellian distribution, which was used for short-plasma resonant mode results. At most the simplified distribution introduces small quantitative differences in results at these plasma lengths. We can identify the various modes by comparing their frequencies, densities, and wave behaviors with those predicted by Berk, et. al.<sup>9</sup> For the negative-energy modes, Table 1 shows the good comparison of frequency and density with the values

predicted by the WKB theory. Figure 2a shows  $\psi(z)$  for these same modes as obtained by our solution of the eigenvalue problem. Figure 2b shows these same modes in the complex  $z$ -plane with the phase angle taken to be  $45^\circ$ , so that a direct comparison may be made with the WKB results.<sup>9</sup> The dotted curve is clearly the  $m = 0$  mode, and the solid curve the  $m = 2$  mode; the dashed curve, the absolute mode, behaves differently from the predicted behavior of any negative-energy mode.

The absolute mode is readily identified by its frequency, density, and wavelength, which compare well with infinite-plasma theory.<sup>8</sup> Also we see in Fig. 3 that the growth rate varies with density in exactly the same manner as in the case of the infinite-plasma at low densities. We note also the completely different behavior of the frequency and density (as the magnetic scale length is changed, Fig. 1) from that of the negative-energy modes.

Thus at long plasma lengths and very long magnetic scale lengths, we are able to identify both the absolute loss-cone mode and the destabilized negative energy waves. We now consider the behavior of these resonant modes as the magnetic scale length is decreased.

We note from Fig. 1 that the magnetic field variation stabilizes all higher- $m$  negative energy modes as predicted by Berk, et al.<sup>9</sup> We also note that the  $m = 0$  mode and absolute mode have a degenerate frequency/density at a magnetic scale length of about  $800 a_i$ . Below this length, one of the roots stabilizes, but the other remains unstable to very short lengths.<sup>10</sup> We term this latter mode the residual mode. The characteristics of this mode may not be the same as the characteristics of the mode at longer scale lengths. This is one clear example of how finite-length effects can cause a mixing of modes.

To understand the behavior of the residual mode as the plasma length is further decreased, we must first study the thermal effects of electrons in our particular model. This model uses a confining potential for the electrons which is essentially a slight distortion of a parabolic potential. In a parabolic potential thermal effects manifest themselves mathematically in the bounce resonance which occur because all particles bounce with the same frequency  $\omega_{be} = \sqrt{T_e/j} / L_p / a_i \sqrt{\frac{M_i T_e}{m_e T_i}}$ , and there is no Landau damping. As already pointed out, for a cold plasma approximation to apply,  $\omega_{be}$  must be much less than  $\omega \approx \Omega_i$ . If we consider a plasma of a length at which the residual mode would stabilize to be  $L_p \approx 20 a_i$ , and if we assume that  $\omega_{be} < .1 \Omega_i$  would be suitable as an approximation for a 'cold' electron plasma, then we find that  $T_e/T_i$  must be less than .0025 in order for this approximation to be valid. We conclude that for most experimental plasmas, we must investigate electron thermal effects.

In a purely parabolically confined plasma, there exists a set of stable plasma oscillations studied by Watson and Harker.<sup>13</sup> Because of the symmetry of  $\psi(z)$ , these oscillations will occur only for even harmonics of  $\omega_{be}$ . At least one of these modes is always destabilized by the ions. Since these bounce modes occur at densities much less than  $\omega_{pi}^2 / \Omega_i^2 = 1$ , we would expect the residual mode characteristics to become like those of the bounce modes as  $\gamma \rightarrow 0$ . This indeed is the case, as indicated in Fig. 4. In fact, in the case of the purely parabolic well, below  $\gamma \approx 10^{-4} \Omega_i$ , the density drops sharply by several orders of magnitude.

One other effect we might expect for a purely parabolically confined plasma is the absence of any (real frequency) mode at  $\omega = m\omega_{be}$ .

Indeed, if we set  $\gamma = .005 \Omega_i$  (so that we are examining the mode where it behaves essentially like a residual mode rather than a bounce mode), we see in Fig. 5a that the frequency does remain between the bounce harmonics, even when it has a small imaginary part.

If we now allow for a departure from purely parabolic potential confinement, as in the model in section II, Landau damping will be present. We first of all expect to see a stabilization of the low-growth-rate electron bounce modes. That this is so is seen in Fig. 4, which shows  $\omega_{pi}^2(\gamma)$  for various amounts of Landau damping. For wells in which thermal particles experience greater than about a ten per cent departure from a parabolic well ( $a = b = .1$ ), these low-density modes have essentially disappeared, and the threshold density becomes characteristic of the residual mode.

Thus we see that in experiments in which the electrons are nearly parabolically confined, the threshold density is an extremely sensitive function of the confining potential, and can vary by several orders of magnitude. However, the growth rates of the low-density modes may be too low to be of physical interest. In our remaining discussion, we wish to focus attention on the residual mode, therefore we eliminate the electron bounce modes by choosing sufficiently strong Landau damping ( $a = b = .1$ ).

With Landau damping, we no longer expect the frequency to be prohibited from existing at the bounce harmonics. This we see from Fig. 5a. We have chosen a  $\gamma = .005 \Omega_i$  to make this comparison (and for subsequently displayed results) because it is large enough so that when there is no Landau damping, the modes behaves essentially like a

residual mode rather than a bounce mode, and yet it is low enough so that when Landau damping is present, it is essentially a threshold curve. We see that the frequency does pass smoothly through the bounce resonance when Landau damping is present (Fig. 5a).

In Figs. 5a and 5b we see that Landau damping has little effect on either frequency or density between the second and fourth bounce harmonics (where  $\omega_{be}$  is large) except when the frequency is near a bounce harmonic, where we expect it to be the greatest (section II). As  $\omega_{be}$  becomes smaller ( $L_p$  becomes larger), the effects of Landau damping for frequencies between the bounce harmonics become larger. The most apparent effect here is the shift of the frequency away from the frequency which would occur without Landau damping.

Because of the strong modulation of the density by the electron bounce resonances, we can determine whether Landau damping is stabilizing or destabilizing only when the frequencies are the same. When the frequency is close to the bounce harmonic with which it would associate itself as  $a$ ,  $b$ , and  $\gamma \rightarrow 0$ , the density is at a minimum, and the mode is most like a destabilized electron bounce oscillation. Here we find Landau damping is stabilizing. On the other hand, when  $\omega$  is not near  $m\omega_{be}$ , we see from the crossings of the  $\omega(L_p)$  curves near  $L_p/a_i = 52, 84$ , and  $113$  that the density is lower when Landau damping is present, indicating a destabilizing effect. These results are consistent with the behavior of the eigenfunction shown in Figs. 6a and 6b, which shows that the perturbed electric field either increases or decreases with Landau damping depending on whether it is destabilizing or stabilizing.

We now consider the behavior of this mode as the plasma length is increased (see Fig. 7). From considerations mentioned earlier, we

expect to see a transition to the straight-line orbit case when  $\omega_{be}/\Omega_i \leq .1$ , which, for  $T_e/T_i = .1$ , corresponds to  $L_p/a_i \approx 140$ .

The connections between the individual bounce harmonic modes are difficult to follow, but they definitely do not join between the low bounce harmonics, and they definitely do join between the tenth and twelfth harmonics. At longer plasma lengths, the modulation of the frequency and density from the electron bounce resonances gradually diminishes, and the straight-line orbit results are recovered. It should be noted that this joining is in no way a consequence of the small  $\gamma$  present in these calculations, as  $\gamma$  is more than an order of magnitude smaller than  $\omega_{be}$ .

Figure 8 shows the behavior of the residual mode growth rate and frequency as a function of plasma density for different plasma lengths. We see that the instability growth rate is largest for short plasmas, reaching a  $\gamma \sim .08 \Omega_i$ . This is to be expected for the negative-energy instability behavior, as the growth rate must go to zero as the plasma length becomes infinite. The lengths were chosen so that the instability occupied the same relative position between different sets of bounce harmonics so as to eliminate bounce structure effects on these results as much as possible.

The behavior of  $\psi(z)$  at different plasma lengths and densities is shown in Fig. 9. Although the ratio of parallel wavelength to plasma length for waves in the ends of the plasma increases in all cases as the plasma is shortened, in no case does the actual wavelength increase, but rather decreases as the plasma length decreases. In the center of the plasma near threshold, Fig. 9a, the behavior is different in the limit of bouncing and non-bouncing electron orbits. When the electrons are

bouncing, the parallel wavelength remains almost constant as the plasma length is varied (cf the cases for  $L_p/a_i = 200$  and  $L_p/a_i = 50$ .) In contrast, in the limit of straight-line orbit electrons, the "wavelength" is proportional to the plasma length. At higher density, Fig. 9b (and higher growth rate), the mode is flute-like in the center of the plasma, and the proportion of plasma length over which the wave-length remains constant is relatively independent of plasma length. So in this limit, the plasma behaves in a way that can be described by equation (34) in contrast to the behavior near threshold. Because of the wave structure near the ends of the plasma, these pictures also lend support to the arguments for careful treatment of the velocity-space distribution function in those regions.

All of these results support the contention that the behavior of the instability at short plasma lengths is dominated by the electron bounce motion, even though there is a ten per cent departure from a parabolic well. It would be entirely reasonable to expect that at least a fifty per cent departure from a parabolic well would be necessary before one could begin to break down the bounce-mode structure between the  $m = 2$  and  $m = 4$  resonances (see Fig 7). Thus the nature of the confinement of the electrons, as well as their thermal properties, will play important roles in determining the frequency and density of resonant modes in short plasmas.

The most important result we find is that for plasma length such that  $2\omega_{be} > \omega$ , there are no unstable resonant modes. For example if we set  $L_p = 50 a_i$ , a length which is able to sustain an instability for  $T_e = .1 T_i$ , and then let  $T_e = T_i$ , we find no physical (real, positive) eigenvalue for any frequency near  $\Omega_i$ . We would like to be able to

generalize this result to apply to all finite plasmas in which the electrons are adiabatic, that is, where  $\omega_{be} \gg \omega$ . We may establish the plausibility of this result by using a model in which the electrons are adiabatic and the perturbed charge density is

$$\rho(\hat{z}) = -\frac{T_i}{T_e} \hat{\omega}_{pi}^2(\hat{z}) (\hat{\psi}(\hat{z}) - \bar{\psi}) \quad (35)$$

where

$$\bar{\psi} = \frac{1}{2\pi} \int_{-\pi}^{\pi} \hat{\psi}(\hat{z}) d\hat{z}$$

is the average potential. This  $\bar{\psi}$ , a constant of integration of the equation of motion for adiabatic electrons, assures that flute modes will not contribute to the perturbed electron charge density. With this  $\rho(\hat{z})$ , we may write Poisson's equation

$$\frac{d^2 \hat{\psi}(\hat{z})}{d\hat{z}^2} - 2\lambda \hat{\psi}(\hat{z}) + \hat{\omega}_p^2(\hat{z}) H(\omega) \hat{\psi}(\hat{z}) - \hat{\omega}_p^2(\hat{z}) \frac{T_i}{T_e} (\hat{\psi}(\hat{z}) - \bar{\psi}) = 0 \quad (36)$$

where  $H(\omega)$  represents the ion term, which we again take in the 'local' approximation.

As we shall see later, flute modes can exist in a plasma with adiabatic electrons, so we must first determine if flute-mode solutions to (36) obtain. By flute mode, we mean that  $\hat{\psi}(\hat{z})$  is essentially constant, despite a large decrease in  $\hat{\omega}_p^2(\hat{z})$  as  $\hat{z}$  increases, until  $\hat{z}$  becomes large enough that  $k_{\perp} \lambda_{De}(\hat{z}) \sim 1$ . So if we write

$$\hat{\psi}(\hat{z}) = \bar{\psi} + \delta \psi(\hat{z})$$

then equation (36) becomes

$$\delta \psi'' - 2\lambda \bar{\psi} - 2\lambda \delta \psi + \hat{\omega}_p^2(\hat{z}) H(\omega) \bar{\psi} + \hat{\omega}_p^2(\hat{z}) H(\omega) \delta \psi - \hat{\omega}_p^2(\hat{z}) \frac{T_i}{T_e} = 0 \quad (37)$$

We now integrate each term of equation (37) from  $-L_0$  to  $L_0$ , where we choose  $L_0$  such that

$$\frac{\hat{\omega}_p^2(L_0)}{\hat{\omega}_p^2(0)} \ll 1 \quad \text{and} \quad \frac{\delta\psi(L_0)}{\bar{\psi}} \ll 1 \quad (38)$$

To lowest order, we get the dispersion relation

$$\left. \begin{aligned} \bar{\omega}_p^2 H(\omega) &= 2\lambda \\ \text{where} \quad \bar{\omega}_p^2 &= \frac{1}{2L_0} \int_{-L_0}^{L_0} \omega_p^2(\hat{z}) \, d\hat{z} \end{aligned} \right\} \quad (39)$$

is the average density of the plasma in the region where  $\delta\psi \ll \bar{\psi}$ . Thus flute modes can exist if a homogeneous-plasma dispersion relation can be satisfied, and the density is the line-averaged density. As we shall see later, our flute-mode results are in agreement with this.

We wish to go to next order in equation (37) to see under what conditions a flute mode can exist. To do this, we use (39) to rewrite (37) as

$$\delta\psi'' + (\hat{\omega}_p^2(\hat{z}) - \bar{\omega}_p^2) H(\omega) \delta\psi - \frac{T_i}{T_e} \hat{\omega}_p^2(\hat{z}) \delta\psi = - (\hat{\omega}_p^2(\hat{z}) - \bar{\omega}_p^2) \bar{\psi} \quad (40)$$

Now if we evaluate this equation at  $L_0$ , we find

$$\frac{\delta\psi(L_0)}{\bar{\psi}} = - \frac{1}{1 + \frac{1}{k_{\perp}^2 \lambda_{De}^2(L_0)} - \frac{\delta\psi''}{2\lambda\delta\psi}} \approx - k_{\perp}^2 \lambda_{De}^2(L_0) = - \frac{T_e}{T_i} \frac{2\lambda}{\hat{\omega}_p^2(L_0)} \quad (41)$$

So we may satisfy our conditions for flute modes, equations (37), if

$$\frac{T_e}{T_i} \frac{2\lambda}{\omega_p^2} \ll \frac{\hat{\omega}_p^2(L_0)}{\omega_p^2} \ll 1 \quad (42)$$

For example, for the Dory-Guest-Harris mode,  $\frac{\omega^2}{\omega_p^2} \sim 100$ , so (42) is readily satisfied. Thus we expect to recover Dory-Guest-Harris modes in the adiabatic-electron limit, and we expect them to have flutelike behavior. On the other hand, near threshold, the negative energy modes, specifically the residual mode, cannot satisfy the condition (42), and thus are not flute-like in behavior. In fact, under no conditions near threshold do we ever observe a flute-like residual mode.

We must therefore examine solutions of (36) for non-flute modes. To do this, we make use of the fact that  $\hat{\psi}(\hat{z})$  must vary on a scale on the order of  $\hat{\omega}_p^2(\hat{z})$  (or faster), in which case we may expand

$$\hat{\omega}_p^2(\hat{z}) \approx \hat{\omega}_{p0}^2 (1 - \hat{z}^2) \quad (43)$$

Poisson's equation then becomes

$$\hat{\psi}''(\hat{z}) + \left[ \hat{\omega}_{p0}^2 \left( H(\omega) - \frac{T_i}{T_e} \right) - 2\lambda - \omega_{p0}^2 \left( H(\omega) - \frac{T_i}{T_e} \right) \hat{z}^2 \right] \hat{\psi}(\hat{z}) = \frac{T_i}{T_e} \hat{\omega}_{p0}^2 \bar{\psi}(1 - \hat{z}^2) \quad (44)$$

For non-flutelike modes, the ion term is

$$H(\omega) = - \sum_n n D_n^i(\lambda) Z \left( \frac{\omega - n\Omega_i}{k_{\parallel} \alpha_{\parallel i}} \right) \approx - D_1^j(\lambda) Z \left( \frac{\omega - \Omega_i}{k_{\parallel} \alpha_{\parallel i}} \right) \quad (45)$$

As the magnitude of  $H(\omega)$  is much less than 1, we may neglect it in comparison with  $T_i/T_e$  for electron temperatures of physical interest ( $T_e \ll T_i$ ). Also because the mode is non-flutelike,  $\bar{\psi} \ll \psi(0) = 1$ , and we may neglect the inhomogeneous term to lowest order. Our differential equation becomes

$$\hat{\psi}''(\hat{z}) - \left[ \hat{\omega}_{p0}^2 \frac{T_i}{T_e} (1 - \hat{z}^2) + 2\lambda \right] \hat{\psi}(\hat{z}) = 0 \quad (46)$$

For  $\hat{z} \ll 1$ , the solution (which vanishes for large  $\hat{z}$ ) is

$$\hat{\psi}(\hat{z}) = A \exp \left[ - \hat{\omega}_{po} \sqrt{\frac{T_i}{T_e}} (1 + k_{\perp}^2 \lambda_{De}^2)^{1/2} \hat{z} \right] \quad (47)$$

which is like a vacuum solution where the Debye shielding distance has been "extended" by the adiabatic electrons. Such a solution is consistent with the approximations of neglecting the  $\hat{z}^2$  term and the inhomogeneous term in (44), and this solution admits no possibility of wave propagation.

We thus conclude that a necessary condition for the existence of unstable modes in plasmas with adiabatic electrons is that the mode exist only at high densities and be flutelike. In earlier work, both flute modes of the Dory-Guest-Harris type and negative-energy modes were predicted to be unstable at short lengths.<sup>10,2</sup> The negative-energy modes were predicted to become stable at sufficiently short plasma lengths because of ion thermal effects (which are properly included in our model, but which do not seem to affect our results greatly). However, the theory used to derive these results depended on  $k_{\parallel} \alpha_e$  being much less than  $\omega$ , and this is not true for the residual mode in short plasmas. In fact, in our model, we do not assume that  $\hat{\psi}(\hat{z})$  is flutelike, but rather let the form of  $\hat{\psi}(\hat{z})$  be determined by the eigenvalue equation. We find that the residual mode near threshold is not flutelike, and can be stabilized at a length dependent on electron temperature. We can therefore write down a minimum-length criterion for stabilization of the residual mode: the plasma is stable against these modes if

$$L_p/a_i \leq 2 \sqrt{\frac{T_e}{T_i} \frac{M_i}{m_e}} \quad (48)$$

## B. Non-Resonant (Flute-Type) Modes

We now turn our attention to a study of two types of flute modes, the Dory-Guest-Harris,<sup>7</sup> and the drift-cone<sup>6</sup> instabilities. While the latter is the more important instability in terms of its potential danger to mirror machines, its characteristics are very similar to those of the Dory-Guest-Harris mode, which we study in detail. We shall first discuss results for the Dory-Guest-Harris instability, with an emphasis on the general characteristics of flute modes, and then we shall focus attention on the drift-cone mode in the plasma parameter region of most interest.

The Dory-Guest-Harris instability occurs in an infinite plasma if the range of  $k_{\perp}$  allows a coupling of ion-cyclotron wave associated with different gyroharmonics, and with our model velocity-space distribution function, can occur only if  $j \geq 3$ . The mode which occurs at lowest density and for smallest  $j$  (corresponding to the smallest loss-cone) occurs at  $\omega = 0$ . The next highest mode occurs at  $\omega \approx 1.2 \Omega_i$ . We examine the properties of these two modes.

It is easier to recover the long-plasma limit numerically for flute modes than for resonant modes, since the principal contribution for flute modes comes from the  $\mu = 0$  component. That we recover this limit is seen in Fig. 10, which shows the density (at a growth rate  $\gamma = .2 \Omega_i$ ) for the  $\omega = 0$  Dory-Guest-Harris mode as a function of plasma length. Results are independent of electron temperature at longer plasma lengths, as one expects for flute modes, and agreement with long-plasma results is good. As the plasma length becomes shorter, electron temperature affects results increasingly, even when  $\omega_{pe}$  is much less than  $\gamma$ . For lengths

below the point where  $\omega_{pe} \sim \gamma$ , we find the density is almost independent of scale length, which we would expect from the adiabatic electron model described above.

We also see changes in the character of the mode from plots of  $\psi(z)$  in Fig. 11. At long lengths, the perturbed potential (scaled to the plasma length) is localized in the center of the plasma. As the plasma length is shortened, the potential remains constant over an increasingly longer proportion of plasma length, corresponding to an increase in the ratio of  $\omega_{pe}$  to  $\gamma$ , and resulting in a slight stabilization because of the resulting 'averaging' of the density over a longer length. Finally, in the regime  $\omega_{pe} > \gamma$ ,  $\psi(z)$  is constant out to where  $k_{\perp} \lambda_{De} \sim 1$ . Since  $\lambda_{De}$ , the electron Debye length, is not a function of plasma length, there is no further increase in plasma density (see Fig. 11).

In contrast with the situation for very long plasmas, there is a slow variation of density with  $T_e$  at short lengths, as seen in Fig. 12. This is primarily a result of the change of the point where  $k_{\perp} \lambda_{De} = 1$ , which results in a variation of the line-averaged density. We may see this from the following model:

$$k_{\perp}^2 \lambda_{De}^2(z_f) = 1 = k_{\perp}^2 a_i^2 \frac{T_e}{T_{ii}} \left[ \frac{\omega_{pi}^2(0)}{\Omega_i^2} \exp(-z_f^2/L_p^2) \right]^{-1}$$

then

$$z_f/L_p = \left\{ \ln \left[ \frac{\omega_{pi}^2(0)}{\Omega_i^2} \frac{1}{k_{\perp}^2 a_i^2} \frac{T_{ii}}{T_e} \right] \right\}^{1/2} \quad (49)$$

Now the average density is

$$\overline{\frac{\omega_{pi}^2}{\Omega_i^2}} = \frac{\omega_{pi}^2(0)}{\Omega_i^2} \frac{L_p}{z_f} \operatorname{erf} \left( \frac{z_f}{L_p} \right) \quad (50)$$

and is constant for constant growth rate. Combining (49) and (50), we get

$$\frac{\omega_{pi}^2(0)}{\Omega_i^2} = \frac{\overline{\omega_{pi}^2}}{\Omega_i^2} \frac{1}{\operatorname{erf}\left(\frac{z_f}{L_p}\right)} \left\{ \ln \left[ \frac{\omega_{pi}^2(0)}{\Omega_i^2} \frac{1}{k_{\perp}^2 a_i^2} \frac{T_{\perp i}}{T_e} \right] \right\}^{1/2} \quad (51)$$

This scaling agrees with that shown in Fig. 12 as long as  $z_f/L_p \geq 1$ .

Let us now examine the behavior of this mode at different growth rates, particularly as  $\gamma \rightarrow 0$ . In Fig. 14, we see a plot of density as a function of  $\gamma$  for various  $\omega_{be}$ , corresponding to various plasma lengths. As  $\gamma$  is decreased, a branch point is eventually reached below which the mode no longer occurs at  $\omega = 0$  and below which the density drops sharply as illustrated by the dotted lines. At these low growth rates, the mode makes a transition to a negative-energy mode, provided one can exist at that plasma length. This is better seen in Fig. 15, which shows the complex frequency variation as the density, the parameter along the curve, is varied. For the mode at a plasma length of  $200 a_i$ , the mode becomes, at low growth rate, a negative-energy mode with a threshold density  $\frac{\omega_{pi}^2}{\Omega_i^2} \approx 1$ . In contrast, the mode for a plasma of length  $20 a_i$ , at which length the residual mode cannot exist, has a frequency, which while not zero, is small, and a threshold density like that of a Dory-Guest-Harris mode. Thus by stabilizing the residual mode (through finite-length effects), we may change the threshold characteristics by a large amount.

The second Dory-Guest-Harris mode, which exists for  $j \geq 6$  and which occurs in an infinite plasma at a frequency  $\omega \sim 1.2 \Omega_i$ , has the same behavior as the  $\omega = 0$  Dory-Guest-Harris mode with one exception mentioned below. First let us consider the variation of density with electron temperature. We see in Fig. 16 that the behavior is exactly the same as

the behavior of the  $\omega = 0$  mode, namely that characterized by equation (51). Figure 17 shows  $\hat{\psi}(z)$  for the same plasma parameters, and almost the same density, for the two different Dory-Guest-Harris modes, and here again the similarity of the flute-mode behavior is apparent.

The variation of density with plasma length is apparently different from that of the  $\omega = 0$  mode, as is seen in Fig. 18. However, this is nothing more than a result of our having chosen a lower growth rate for the second mode. When the growth rate is lower, the mode takes on the characteristics of the residual mode as long as the plasma is sufficiently long for that mode to exist. The same behavior would have obtained had we chosen a growth rate  $\gamma \leq .08 \Omega_i$  for the  $\omega = 0$  mode (except that the  $\omega = 0$  mode couples into the residual mode at  $\omega \sim \Omega_i$ , while the second mode seems to couple into the equivalent mode at  $\omega \sim 2\Omega_i$ ). Conversely, had we chosen a higher growth rate for this second Dory-Guest-Harris mode, the behavior would have been the same as that of the  $\omega = 0$  mode.

We now turn our attention to the drift-cone instability. This instability, first examined in an infinite, homogeneous plasma by Post and Rosenbluth and by Mikhailovskii<sup>6</sup> is, like the Dory-Guest-Harris mode, a flute mode in a homogeneous plasma. In a finite plasma, it also shares many of the properties of the Dory-Guest-Harris mode. One principal difference in the characteristics of the two modes is that the drift-cone mode can have much higher growth rates than the Dory-Guest-Harris mode, in fact, greater than the ion cyclotron frequency. Because of these high growth rates, the mode is potentially very dangerous for mirror-contained plasmas.

In the high growth rate regime (where the mode has flutelike behavior), the variation of density (at a constant growth rate) with plasma length is the same as that of the Dory-Guest-Harris mode pictured in

Fig. 10; in other words, as the plasma is shortened, the instability becomes less unstable in the sense that a higher density is required for a given growth rate. In the low growth rate regime, it also behaves like the Dory-Guest-Harris instability shown in Fig. 18, that is, the density decreases as the plasma length is decreased until a certain point where the density rises sharply. The variation with electron temperature is also identical with that of the Dory-Guest-Harris mode: when  $\omega_{be}$  is much less than the wave frequency, the results are essentially independent of electron temperature, while in the opposite limit ( $\omega_{be} \gg \omega$ ) the flute-mode behavior of the type shown in Figs. 12 and 16 for the Dory-Guest-Harris mode obtains.

The variation of density with growth rate for two different plasma lengths is shown in Fig. 19a. As mentioned above, this is also similar to the Dory-Guest-Harris mode, except for the higher growth rates of the drift-cone mode. Notice that the drift cone mode at  $L_p/a_i = 50$  does not couple into the residual mode which exists at that length at lower density (see dashed curve). By contrast, the curve for a plasma length of  $210 a_i$  shows the transition of the drift-cone mode into the residual mode as the density becomes small. This curve should be compared with the same curve in the absence of a radial density gradient (Fig. 8); below the transition, the mode in Fig. 19 takes on the same properties as the mode in Fig. 8. At larger values of  $k_\perp$ , the drift-cone mode occurs at higher frequencies, and, although its threshold density is higher than for lower  $k_\perp$ , it can occur at higher growth rates than the lower  $k_\perp$  drift-cone mode. This is illustrated by the third curve in Fig. 19a, which shows results for  $k_\perp a_i = 10$ . The corresponding frequencies for these curves are shown in Fig. 19b.

It is also true that the most unstable  $k_{\perp}$  for a Dory-Guest-Harris mode does not coincide with the most unstable  $k_{\perp}$  for either of the other two types of residual and drift-cone modes. Nevertheless, we may find ranges of  $k_{\perp}$  in which all of the modes studied are unstable. If we now examine one mode, say the Dory-Guest-Harris mode with such a  $k_{\perp}$ , and if we now 'turn on' the drift-cone mode by increasing the radial density gradient, we find that the character of the mode makes a smooth transition from a Dory-Guest-Harris mode to a drift-cone mode. This is illustrated in Fig. 20, which shows frequency as a function of density for different values of radial density gradient. We must conclude that in a short plasma, no instability exists as a separate entity if another unstable mechanism can exist, and that the instability will always behave according to whatever instability mechanism is 'strongest' with the given plasma parameters.

## IV. SUMMARY AND CONCLUSIONS

In this paper, we have reported results from calculations employing a model which is valid in short as well as long plasmas, at high as well as low electron temperatures, and for flute modes as well as non-zero  $k_{\parallel}$  modes. In regimes in which results have been calculated previously using other theories, we get good agreement with the one exception mentioned. Moreover, our results are internally consistent.

Of course a model is used, and any model is limited by the number of physical effects which are included. We have, nevertheless, included in our model the necessary effects included in previous theoretical models, namely the ones which should answer the questions concerning the stability of short, mirror-contained plasmas. In addition, we have included electron temperature effects which were not included in previous models, and we have found these effects to be important, especially in short plasmas.

Our results consistently show that no unstable resonant mode exists in a short, mirror-contained plasma, and that the minimum unstable length for such a plasma is dependent on electron thermal properties. An analytical model used to interpret these results also leads to the same conclusion - that no real-density eigenmode can exist in a short plasma with adiabatic electrons, that is, when the thermal electron bounce frequency is greater than the wave frequency.

Of course we are still left with the spectre of the existence of the high-growth-rate flute modes in mirror plasmas, no matter how short the plasma. However, it may be important that this flute mode must exist as a separate entity, rather than as an instability with mixed

properties. For instance, finite- $\beta$  effects affect resonant modes very little, while they seem to have a much larger effect on flute modes. Thus there is some reason to look for stabilizing effects when only one type of unstable mode exists.

One direction to pursue the matter is with finite- $\beta$  effects. Indeed, techniques using this basic model but incorporating finite- $\beta$  effects have already been reported, and more work awaits the completion of this present study.

Whether or not some regime of complete stabilization can be attained is still a matter very much open to question. At least we have found that the threshold density for the onset of instabilities in short mirror plasmas is higher than predicted by previous results, and these results should serve as a guide for scaling experiments to test this.

#### ACKNOWLEDGMENTS

The authors wish to acknowledge the generous support of the Max-Planck Institut für Plasmaphysik, Garching bei München, in the form of logistical and computing support for one of us (CB) to enable us to study the effects of electron Landau damping, and to allow collaboration between two of us (JEM and CB) in the writing of parts of this paper during January - April, 1973.

The authors are also indebted to Drs. H. L. Berk and L. D. Pearlstein of Lawrence Laboratory, Livermore, for their direction and aid in the derivation of the perturbed ion density term with presence of magnetic field variations. We also wish to thank these experts for numerous discussions of our results and for providing incentives for improvements in our model.

We also wish to acknowledge helpful discussion with Drs. CJH Watson, J. G. Cordey, and J. D. Callen, which were very helpful.

## LIST OF REFERENCES

1. C. O. Beasley, Jr., W. M. Farr, H. Grawe, Phys. Fluids 13, 2563 (1970).
2. D. E. Baldwin, C. O. Beasley, Jr., H. L. Berk, W. M. Farr, R. C. Harding, J. E. McCune, L. D. Pearlstein, and A. Sen in "Plasma Physics and Controlled Nuclear Fusion Research" (International Atomic Energy Agency, Vienna, 1971) Vol. II, p. 735.
3. G. E. Guest and R. A. Dory, Phys. Fluids 8, 1853 (1965).
4. H. L. Berk and L. D. Pearlstein, Phys. Fluids 14, 1810 (1971).
5. J. E. McCune, USAEC Report ORNL-TM-2258, Oak Ridge National Laboratory, (October 1972).
6. A. B. Mikhailovskii, Nuclear Fusion 2, (1962) and R. F. Post and M. N. Rosenbluth, Phys. Fluids 9, 730 (1966).
7. R. A. Dory, G. E. Guest, and E. G. Harris, Phys. Rev. Letters 14 131 (1965).
8. C. O. Beasley and J. G. Cordey, Plasma Physics 10, 411 (1968).
9. H. L. Berk, L. D. Pearlstein, J. D. Callen, C. W. Horton, and M. N. Rosenbluth, Phys. Rev. Letters 22, 876 (1969).
10. H. L. Berk, L. D. Pearlstein, and J. G. Cordey, Phys. Fluids 15, 891 (1972).
11. W. M. Tang, L. D. Pearlstein and H. L. Berk, Phys. Fluids 15, 1153 (1972).
12. P. H. Rutherford and E. A. Frieman, Phys. Fluids 10, 1007 (1967).
13. C. J. H. Watson, "The Electrostatic Oscillations of Non-Uniform Plasmas," Doctoral Thesis, Oxford University, UKAEA Report CLM-M40 (1964); Kenneth J. Harker, Phys. Fluids 8, 1846 (1965).
14. D. E. Baldwin and G. Rowlands, Phys. Fluids 9, 2444 (1966).

Table 1. Comparison of Long-Plasma Theory  
with Numerical Results

Absolute mode	$k_{\perp} a_i = 2.25, j = 5 \quad T_{\perp i} = T_{\parallel i} \quad T_e = .1 T_i$
	$\gamma = .016 \Omega_i$
Infinite, homogeneous theory	$\omega = .939 \Omega_i \quad \omega_{pi}^2 / \Omega_i^2 = .97 \quad \frac{k_{\parallel} \alpha_{\parallel}}{\Omega_i} = .035$
$L_p / a_i = 900 \quad L_m / a_i = 10^4$	$\omega = .937 \Omega_i \quad \omega_{pi}^2 / \Omega_i^2 = .965 \quad \frac{k_{\parallel} \alpha_{\parallel}}{\Omega_i} = .035$
$m = 0$ mode $L_p / a_i = 400$	
Berk, et al. ( $L_m = \infty$ )	$\omega = .802 \Omega_i \quad \omega_{pi}^2 / \Omega_i^2 = 4.57$
$L_m / a_i = 10^4$	$\omega = .797 \Omega_i \quad \omega_{pi}^2 / \Omega_i^2 = 5.34$
$m = 2$ mode $L_p / a_i = 400$	
Berk, et al. ( $L_m = \infty$ )	$\omega = .931 \Omega_i \quad \omega_{pi}^2 / \Omega_i^2 = 1.29$
$L_m / a_i = 10^4$	$\omega = .932 \Omega_i \quad \omega_{pi}^2 / \Omega_i^2 = 1.22$

## LIST OF FIGURES

- Fig. 1a Variation of Frequency with Magnetic Scale Length
- Fig. 1b Variation of Density with Magnetic Scale Length
- Fig. 2a  $\hat{\psi}(z)$  Resonant Eigenmodes in Long Plasmas
- Fig. 2b  $\hat{\psi}(z)$  along  $z = (1 + i z_r)$
- Fig. 3 Growth Rate versus Density of the Absolute Loss-Cone Instability
- Fig. 4 Density Versus Growth Rate for Various Amounts of Landau Damping
- Fig. 5a Frequency of the Residual Mode Versus Plasma Length
- Fig. 5b Density of the Residual Mode Versus Plasma Length
- Fig. 6a  $\hat{\psi}(z/L_p)$  for  $\omega$  Not Near Its Bounce Resonance
- Fig. 6b  $\hat{\psi}(z/L_p)$  for  $\omega$  Near Its Bounce Resonance
- Fig. 7a Frequency of the Residual Mode Versus Plasma Length  
(With Landau Damping)
- Fig. 7b Density of the Residual Mode Versus Plasma Length (With  
Landau Damping)
- Fig. 8 Frequency and Growth Rate of Residual Mode at Different Plasma  
Lengths
- Fig. 9a Residual Mode  $\hat{\psi}(z)$  For Various Plasma Lengths Near Threshold
- Fig. 9b Residual Mode  $\hat{\psi}(z)$  For Various Plasma Lengths at High Density  
(High  $\gamma$ )
- Fig. 10 Density Versus Plasma Length for the  $\omega = 0$  Dory-Guest-Harris  
Mode with  $\gamma = .2 \Omega_i$
- Fig. 11  $\hat{\psi}(\hat{z})$  Dory-Guest-Harris Eigenmodes at Various Plasma Lengths
- Fig. 12 Density Versus Electron Temperature for the  $\omega = 0$  Dory-Guest-Harris  
Mode with  $\gamma = .2 \Omega_i$
- Fig. 13  $\hat{\psi}(\hat{z})$  Dory-Guest-Harris Eigenmodes at Various Electron Temperatures

## LIST OF FIGURES (Cont.)

- Fig. 14 Density Versus Growth Rate for Various Plasma Lengths, Showing Transitions to  $\omega \neq 0$  Modes
- Fig. 15 Complex Frequencies for Eigenmodes of Lowest Dory-Guest-Harris Mode at Two Different Plasma Lengths
- Fig. 16 Density as a Function of Electron Temperature for  $\omega = 1.2 \Omega_i$  Dory-Guest-Harris Mode,  $\gamma = .1 \Omega_i$
- Fig. 17  $\hat{\psi}(z)$  Dory-Guest-Harris Eigenmode,  $\omega = 0$  and  $\omega \approx 1.2 \Omega_i$
- Fig. 18 Frequency and Density versus Plasma Length,  $\omega = 1.2 \Omega_i$  Dory-Guest-Harris Mode
- Fig. 19a Variation of Growth Rate with Density at Different Plasma Lengths, Different  $k_{\perp}$
- Fig. 19b Variation of Frequency with Density at Different Plasma Lengths, Different  $k_{\perp}$
- Fig. 20 Frequency and Growth Rate versus Density for Combination Dory-Guest-Harris - Drift-Cone Modes

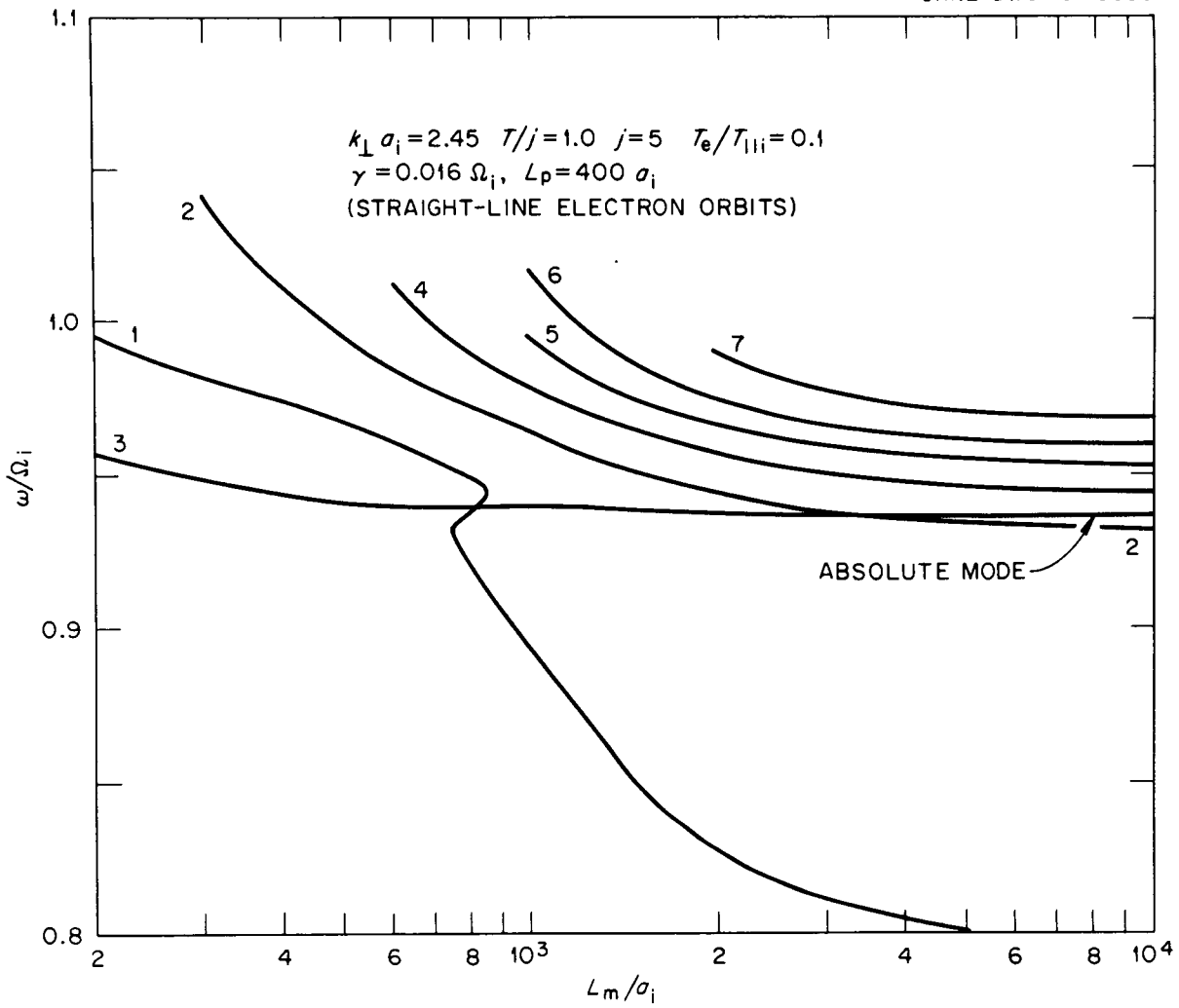


Fig. 1a

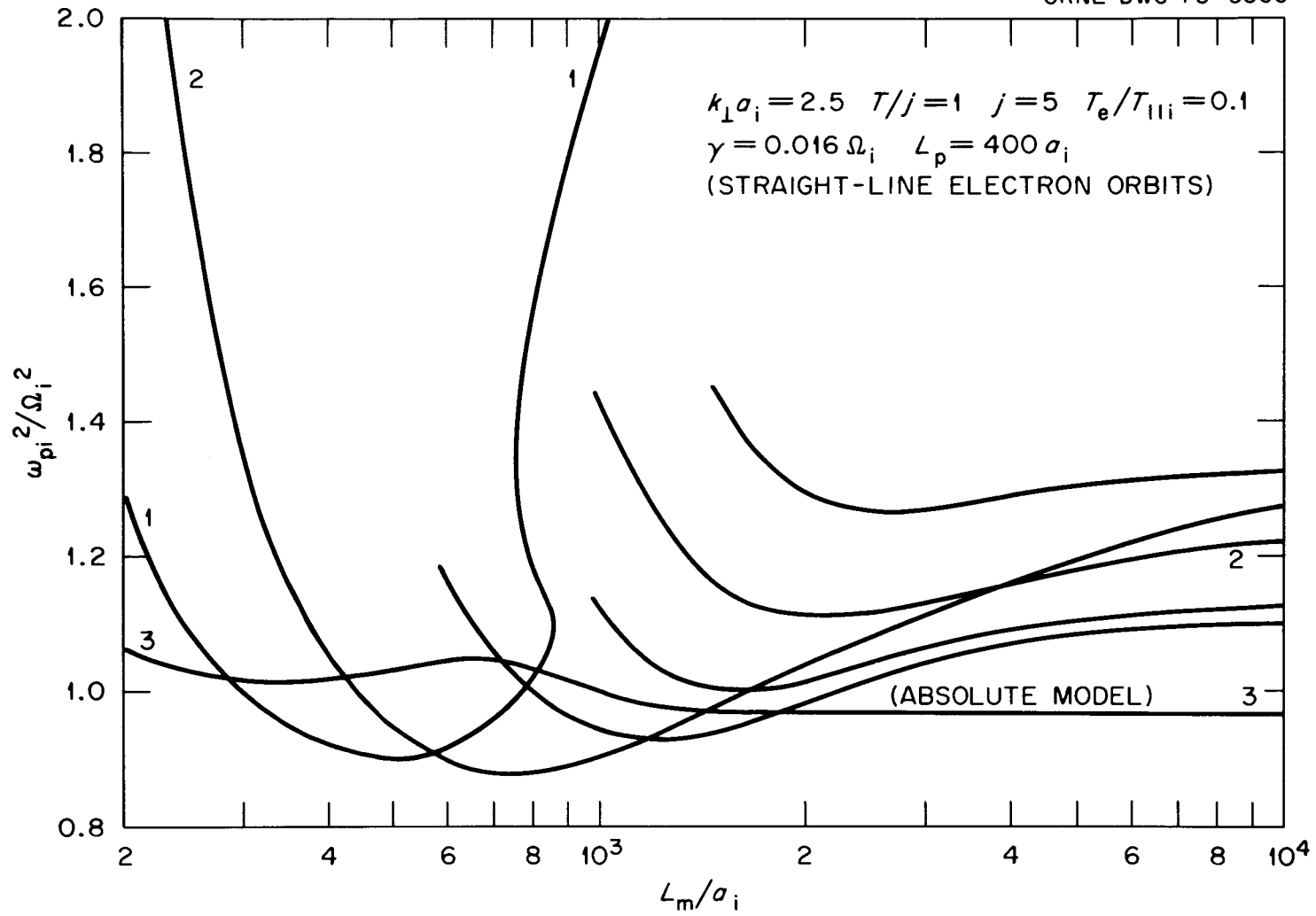


Fig. 1b

ORNL-DWG 73-5378

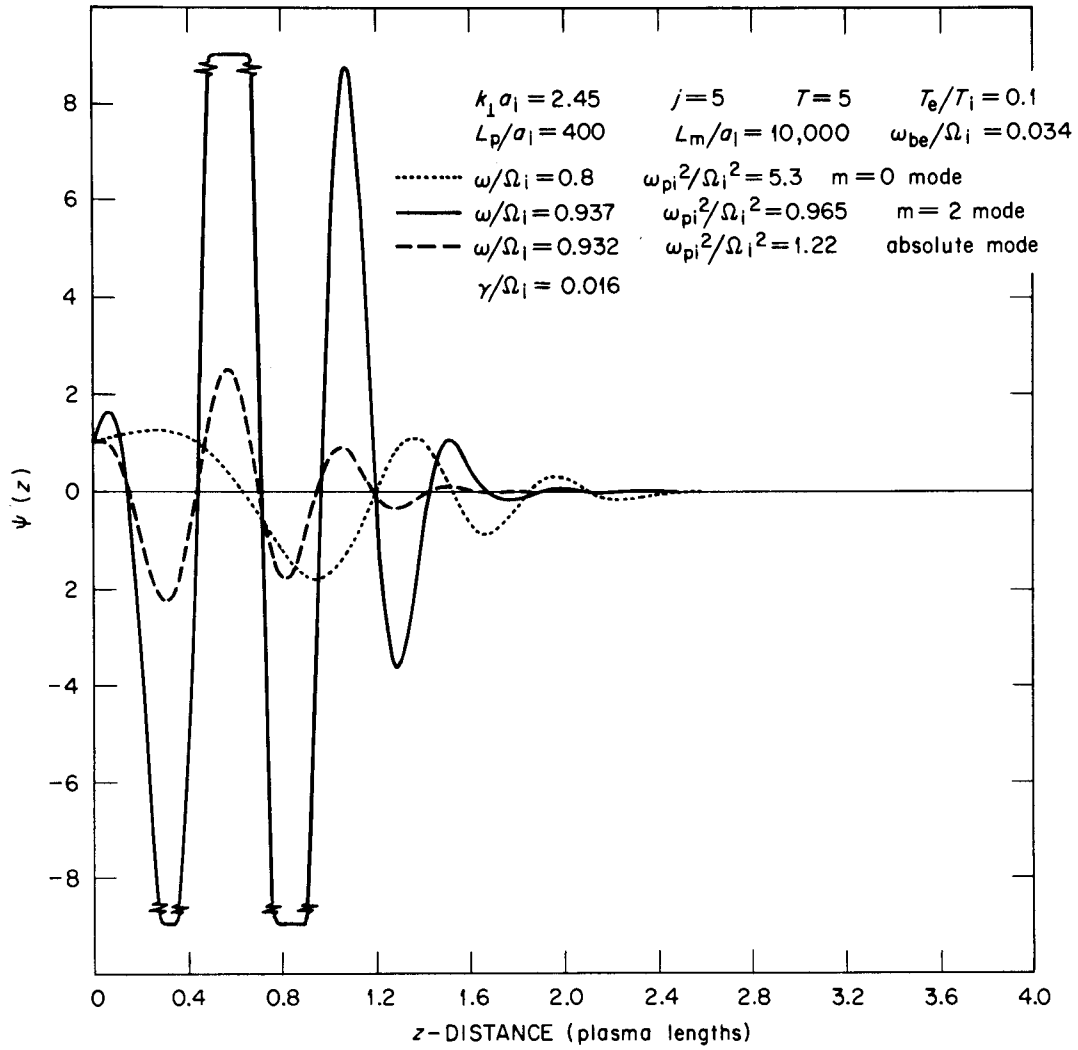


Fig. 2a

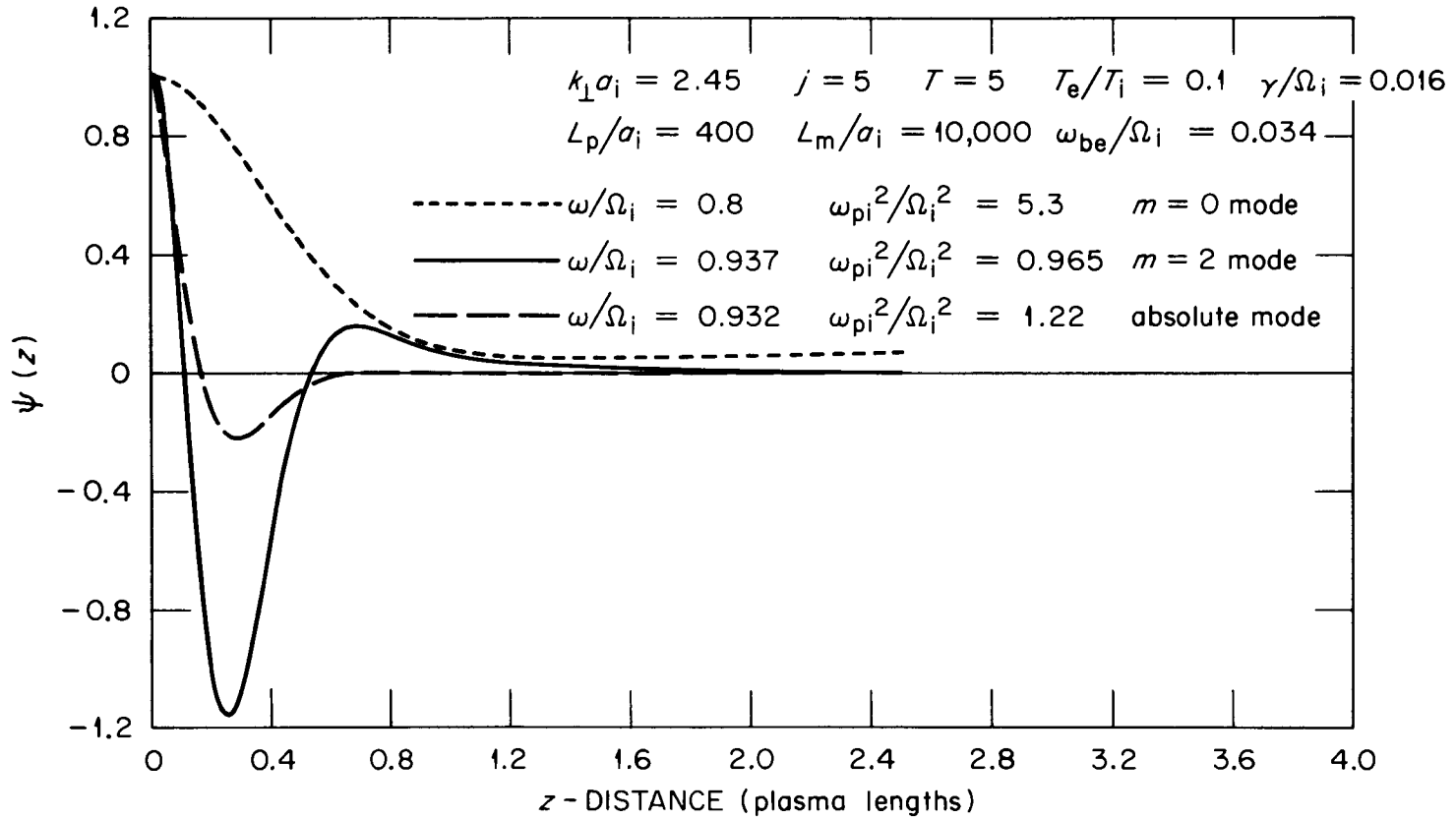


Fig. 2b

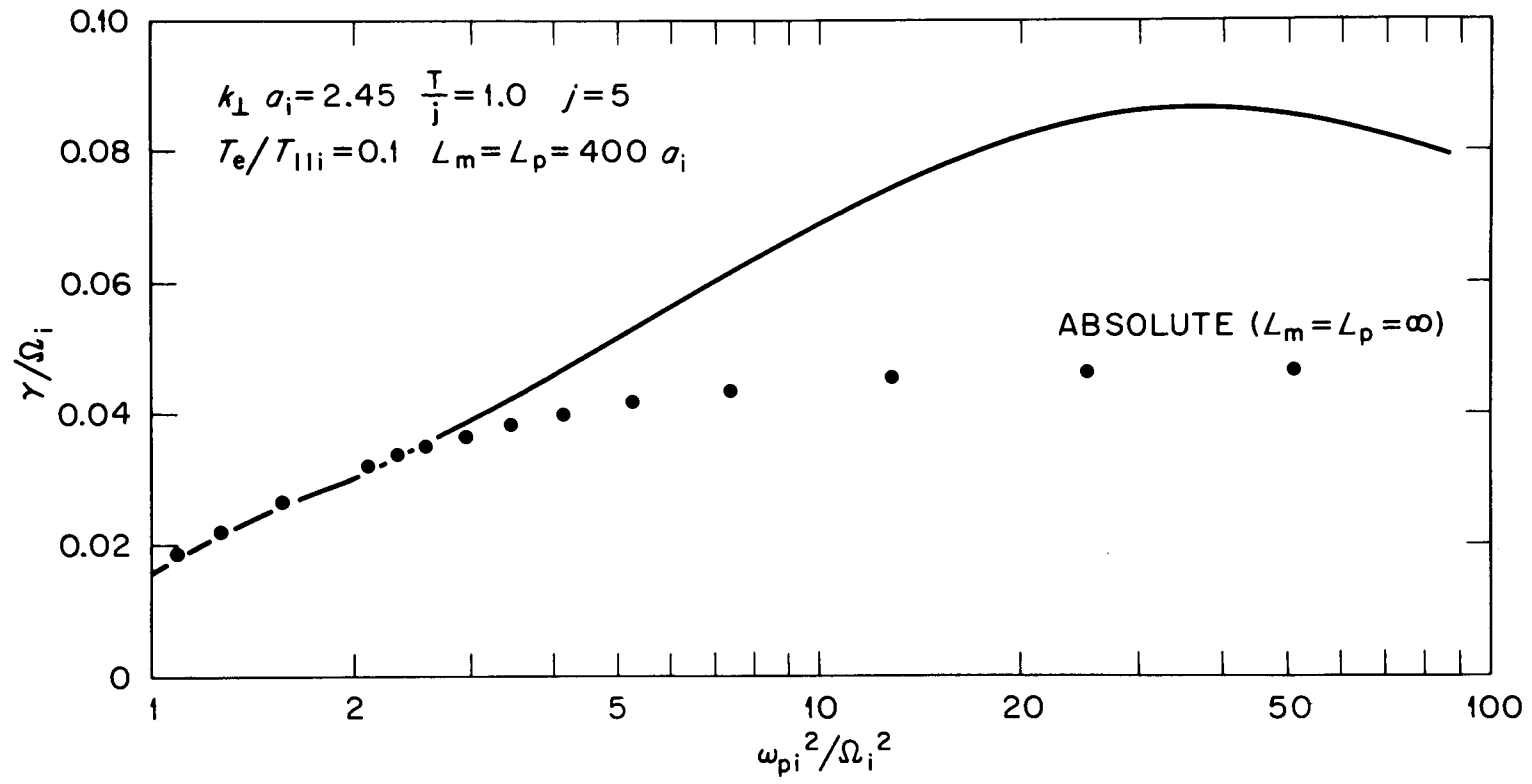


Fig. 3

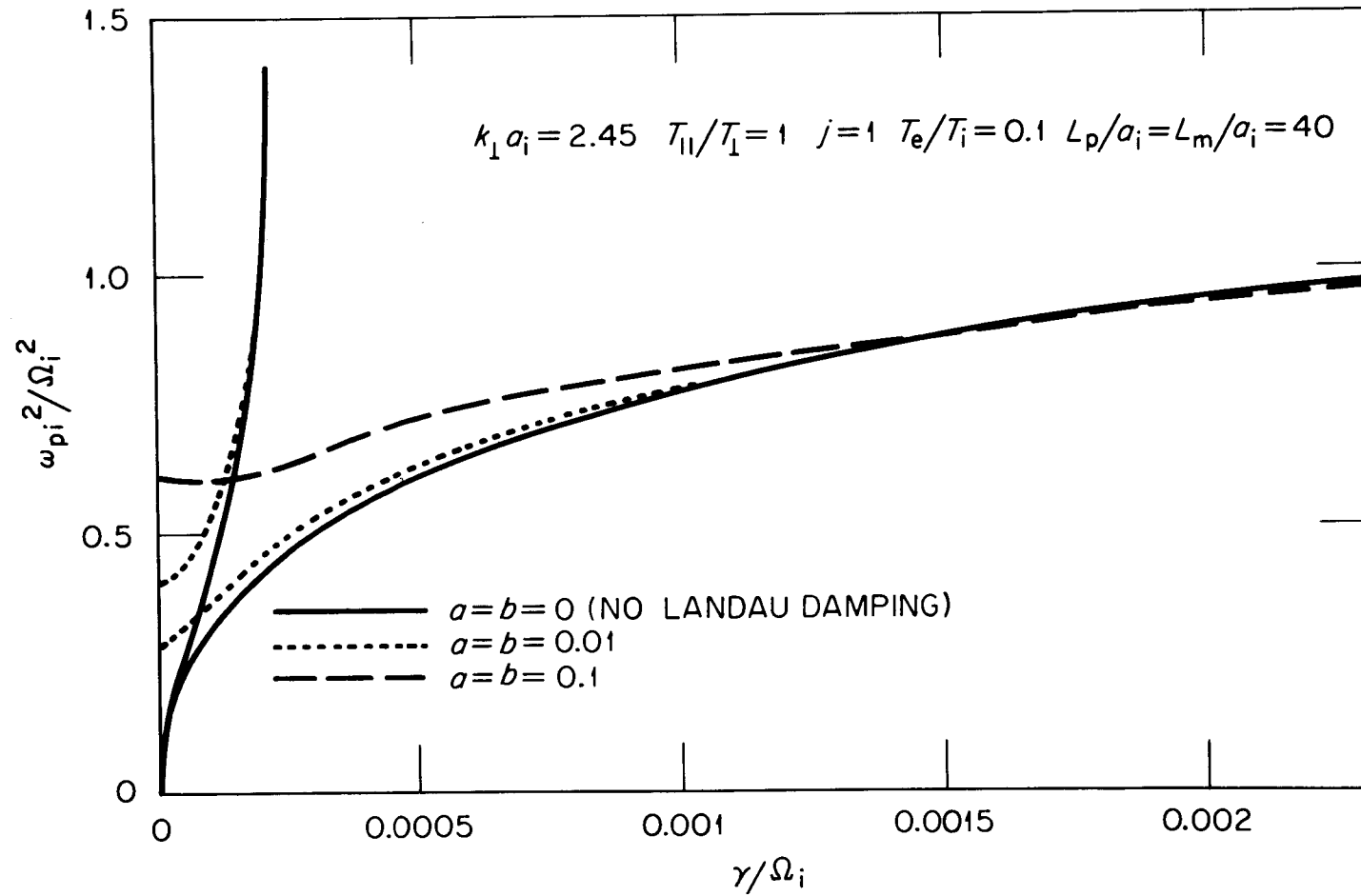


Fig. 4

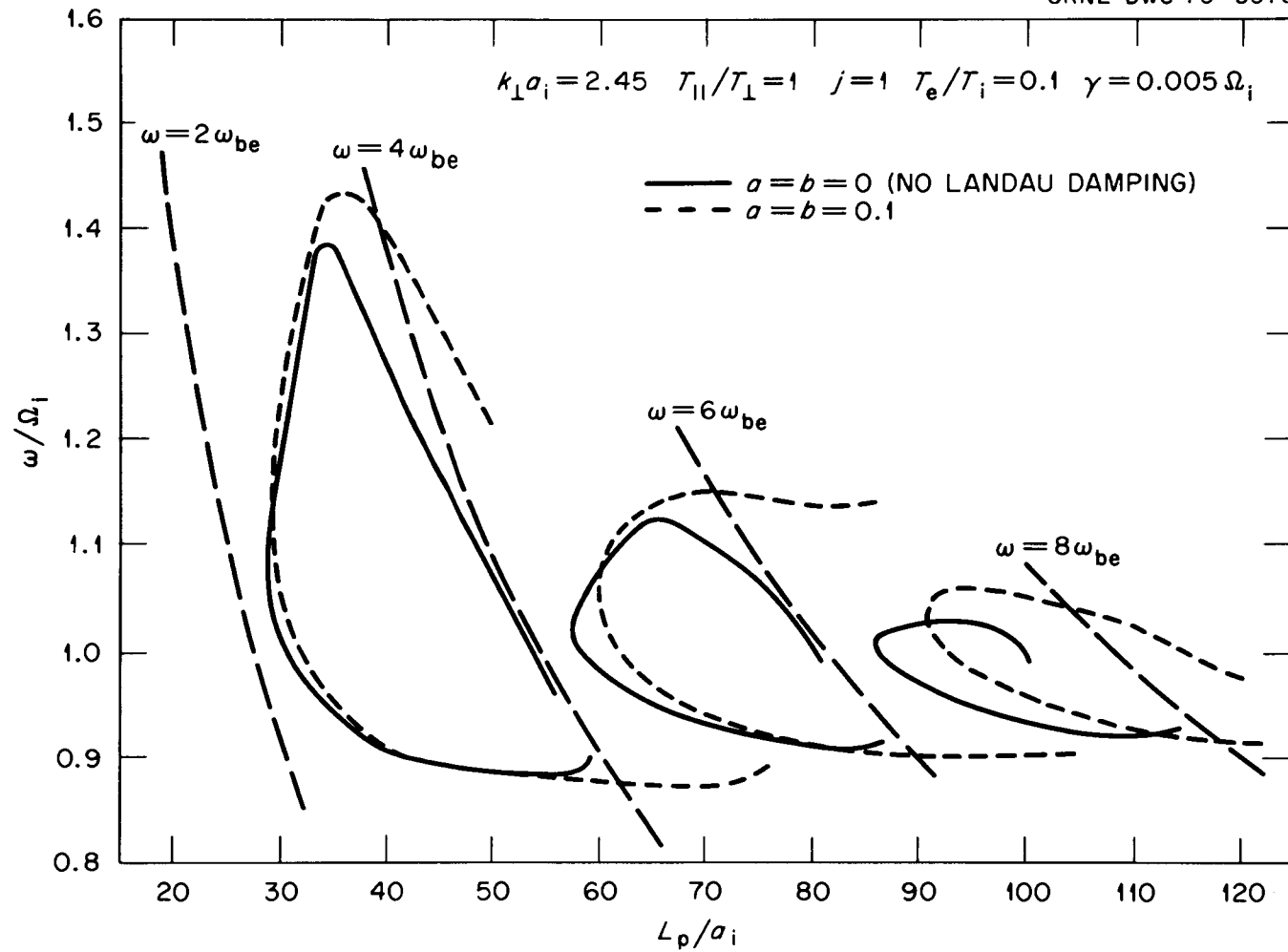


Fig. 5a

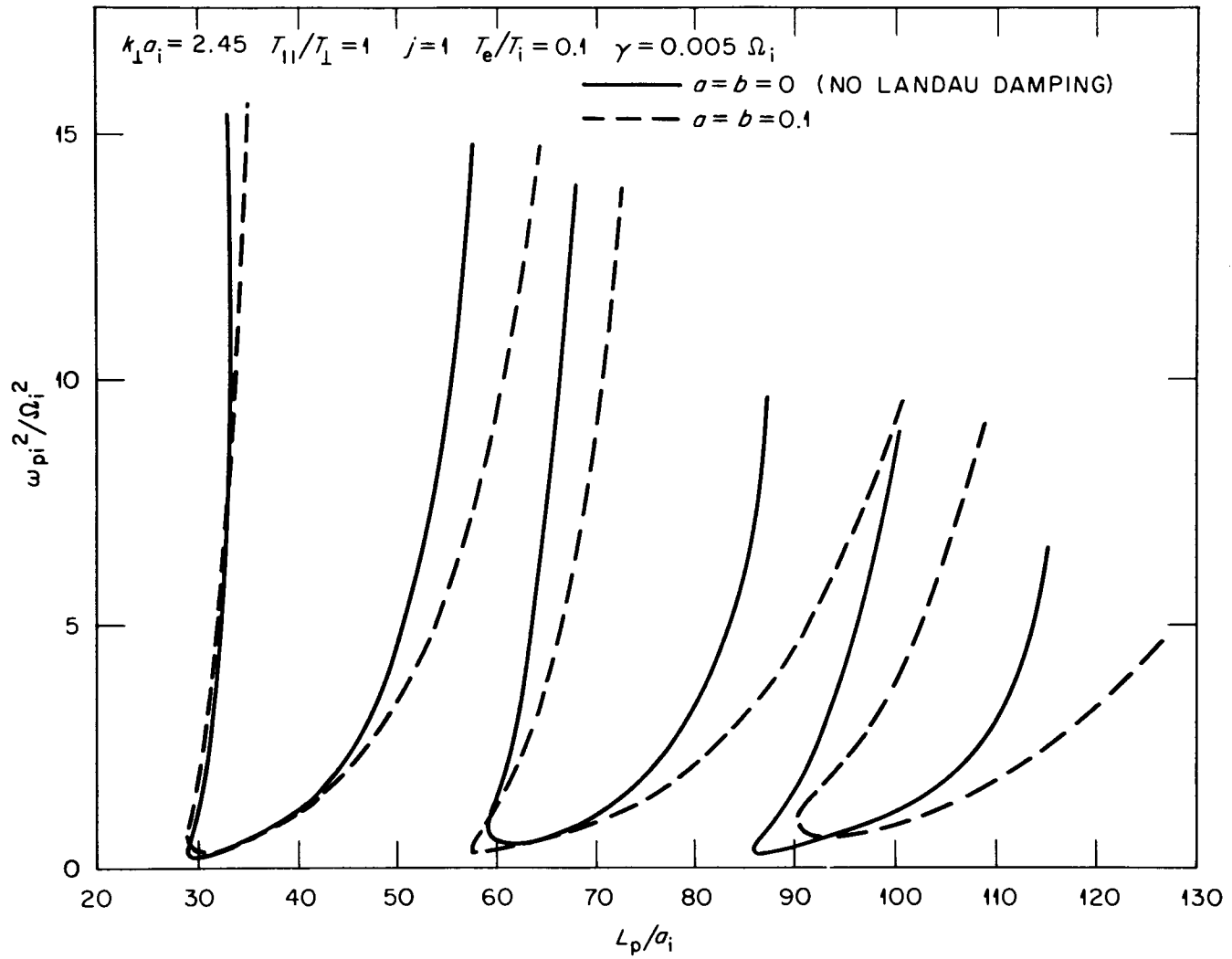


Fig. 5b

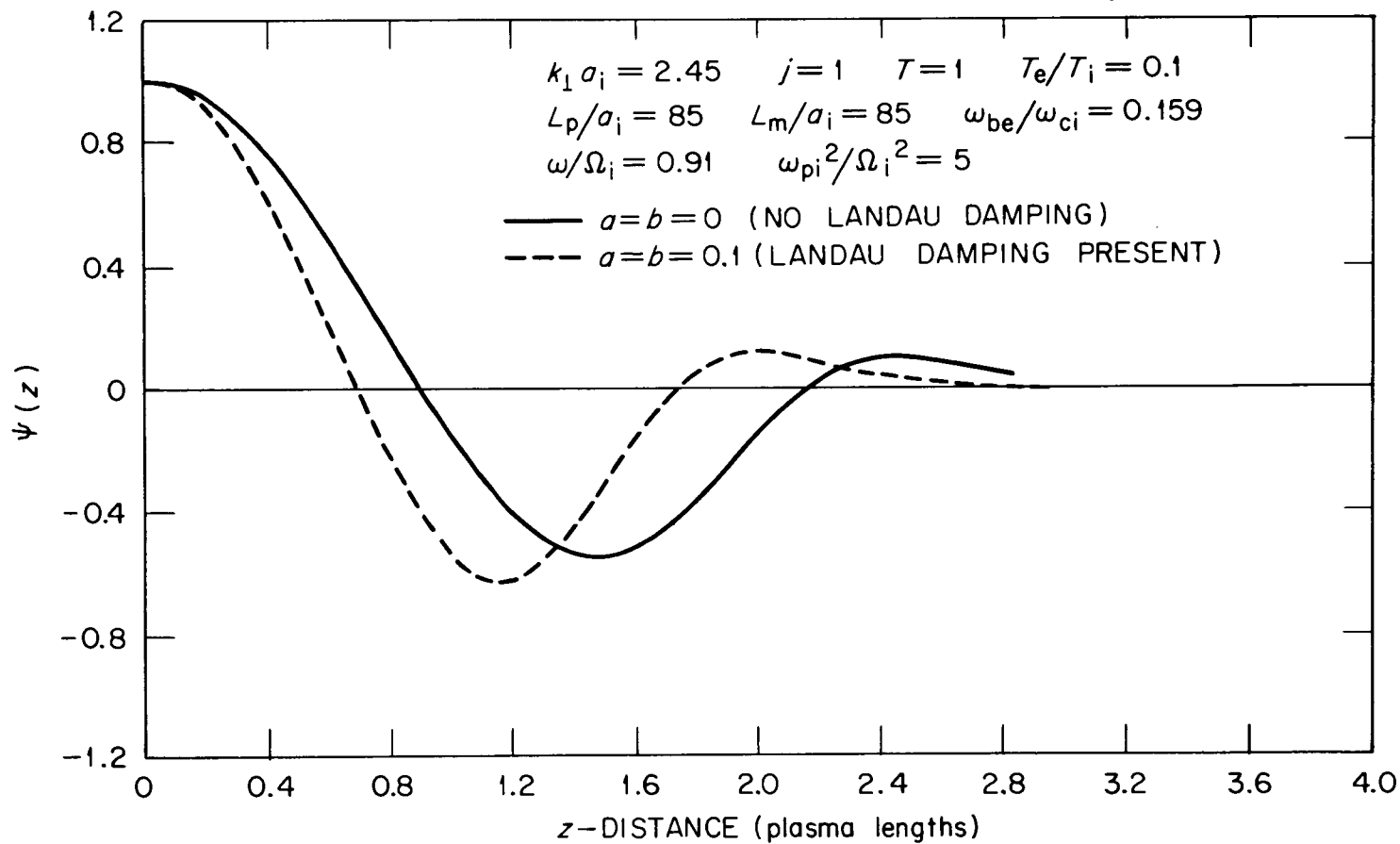


Fig. 6a

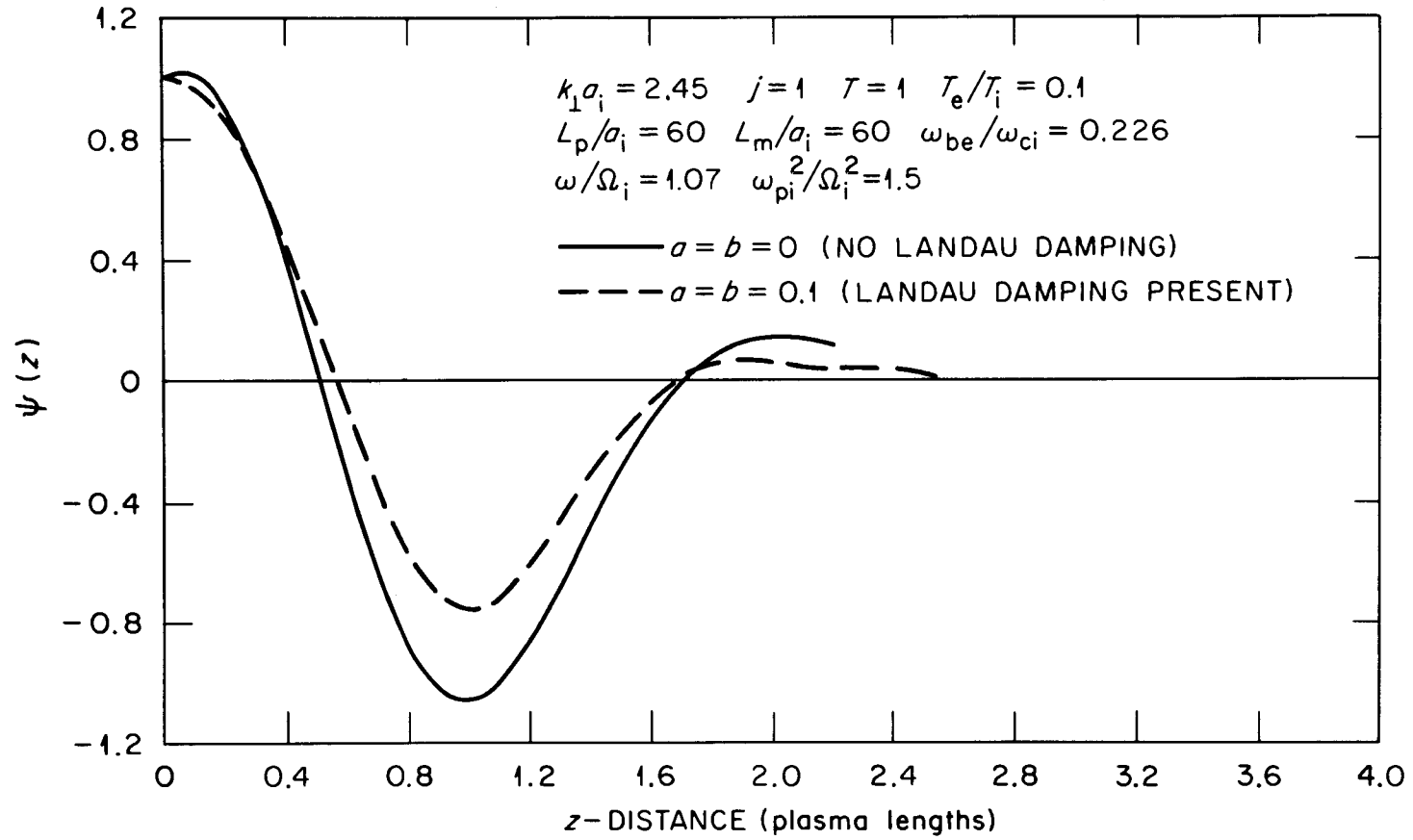


Fig. 6b

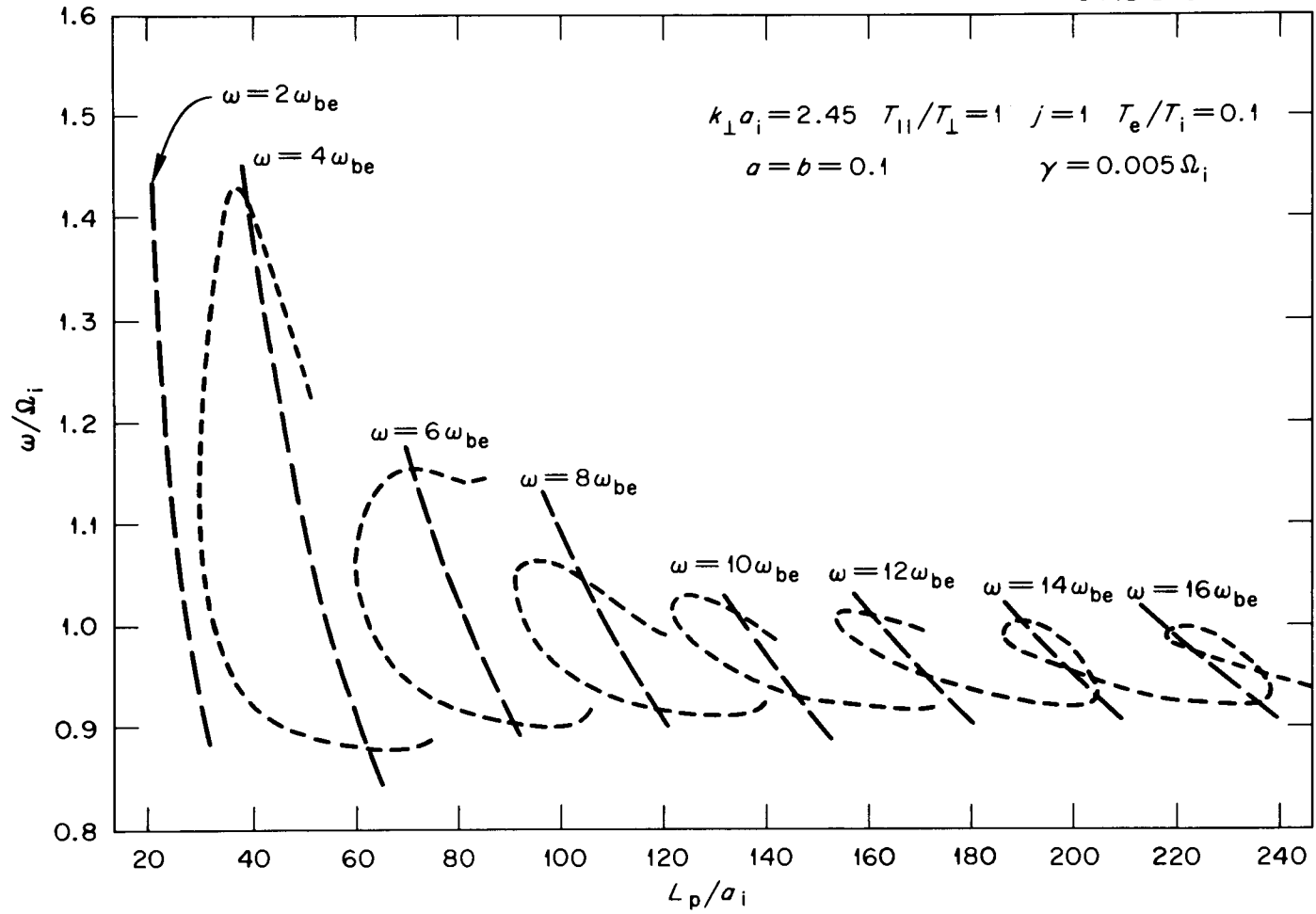


Fig. 7a

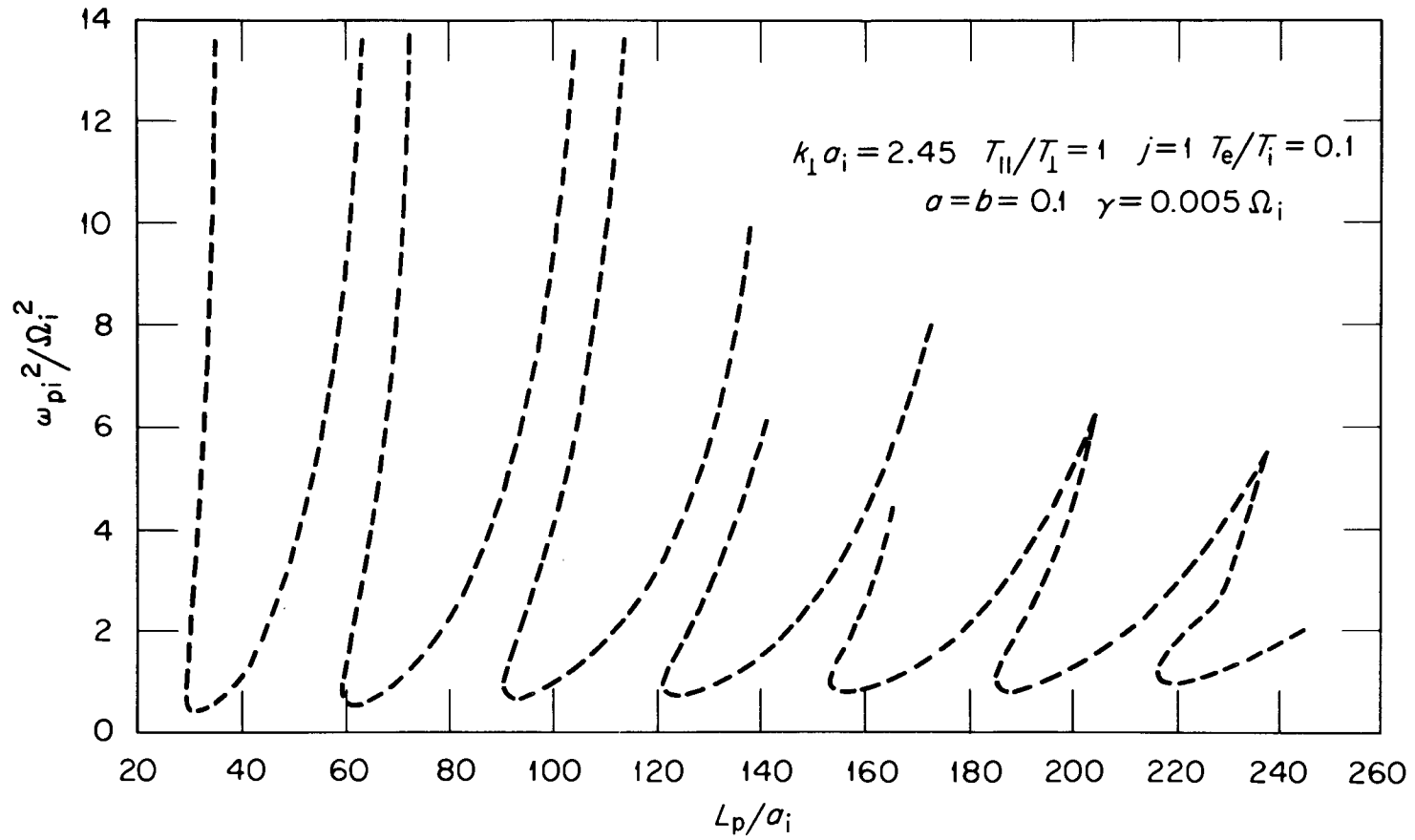


Fig. 7b

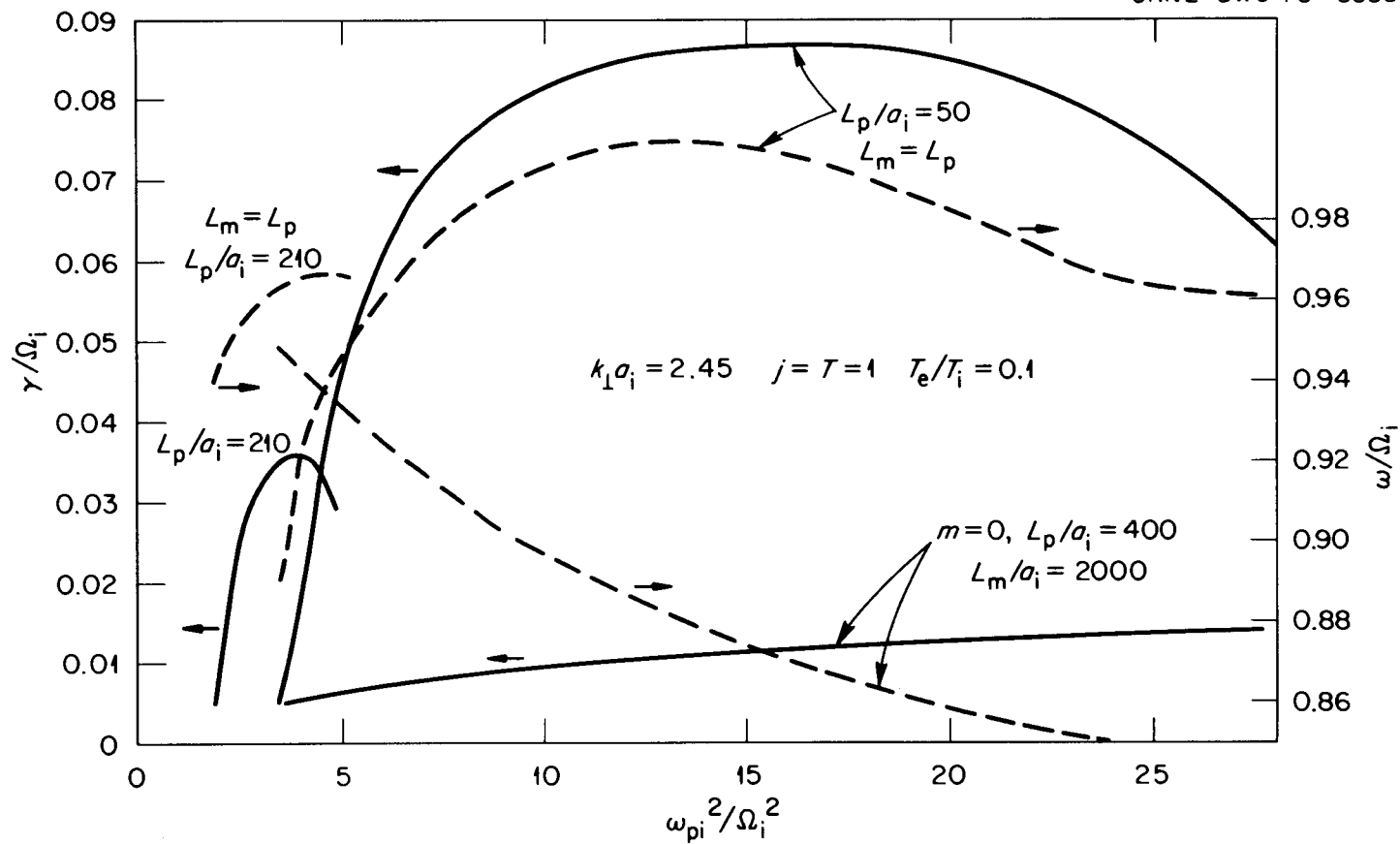


Fig. 8

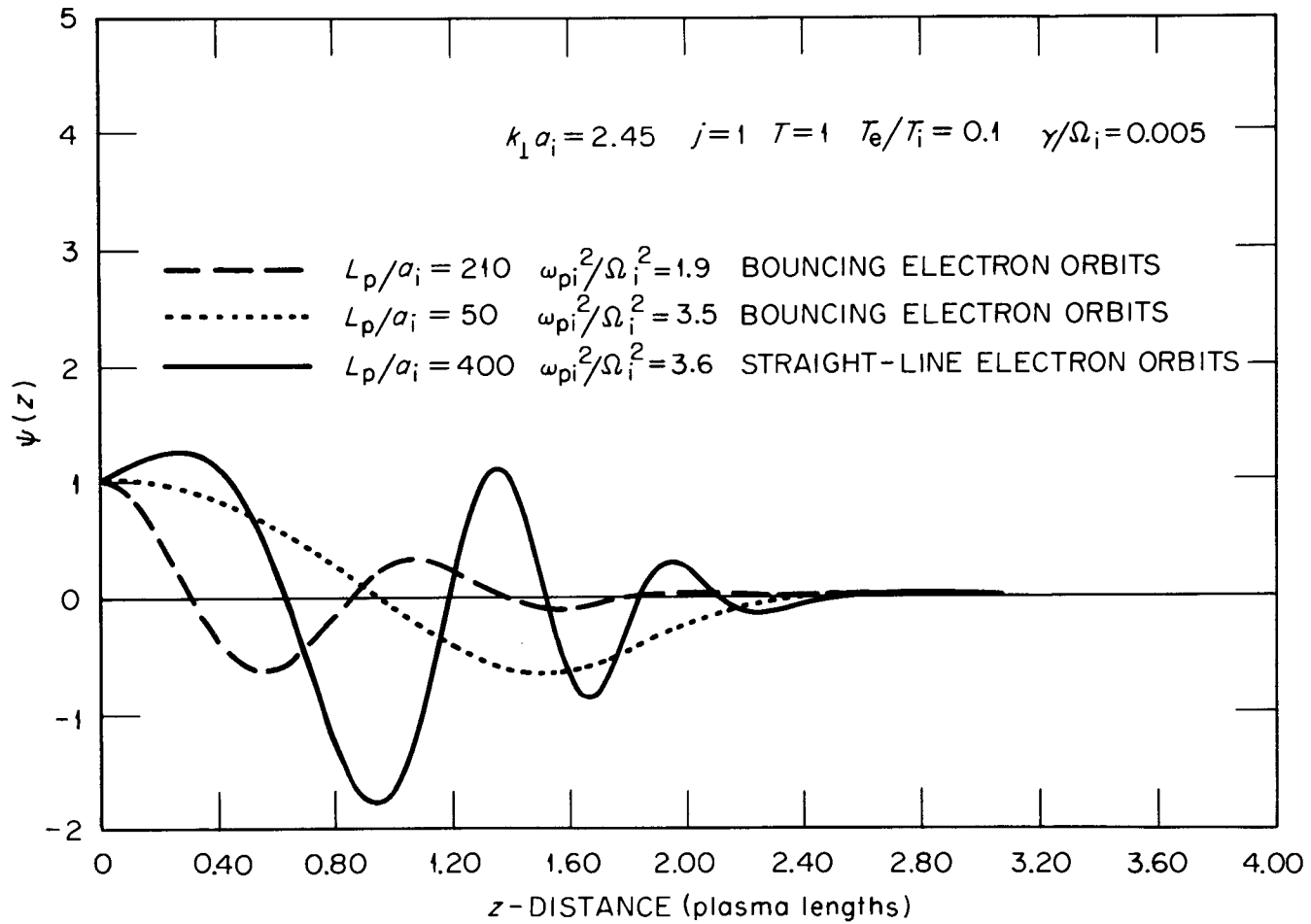


Fig. 9a

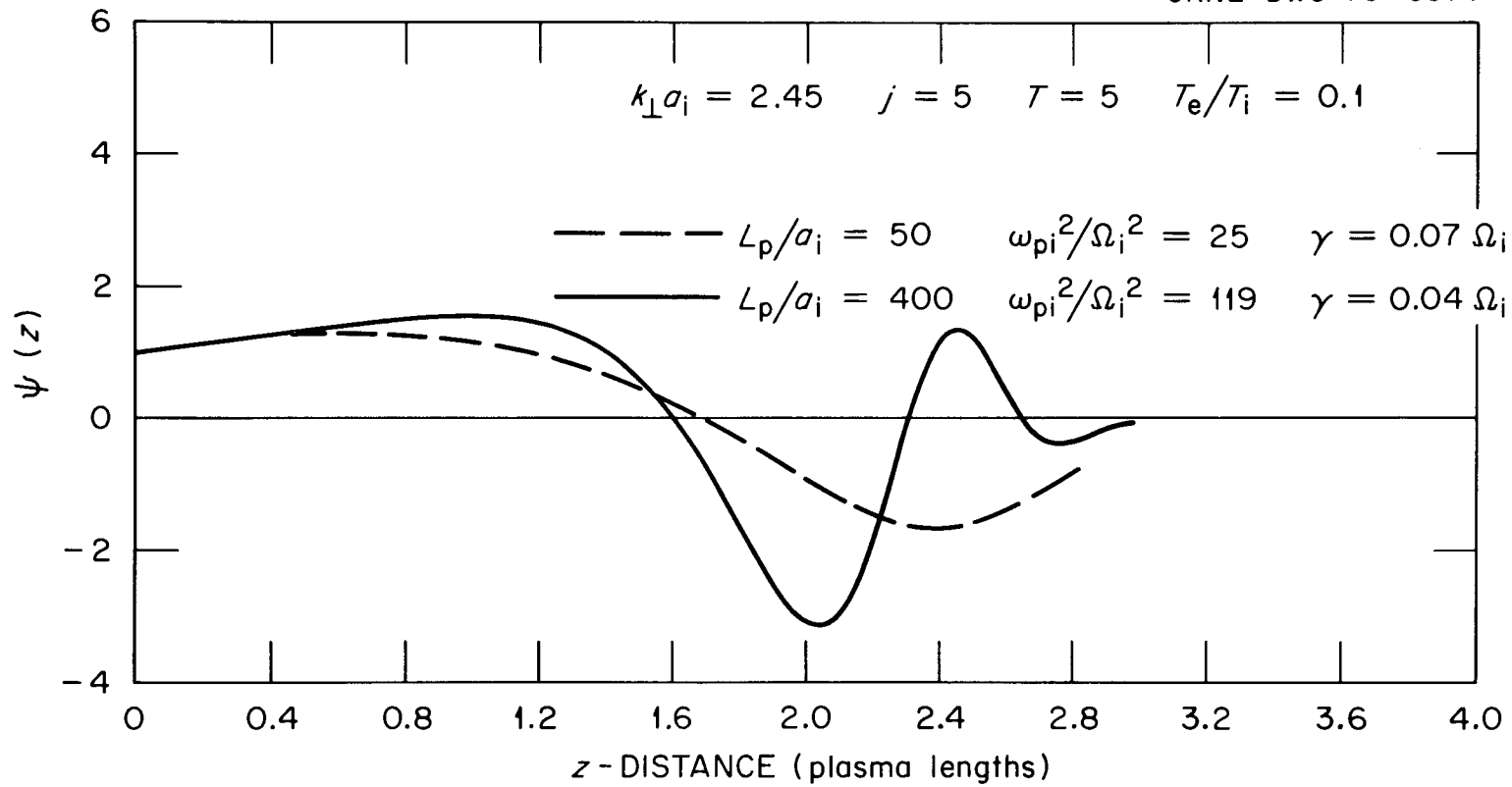


Fig. 9b

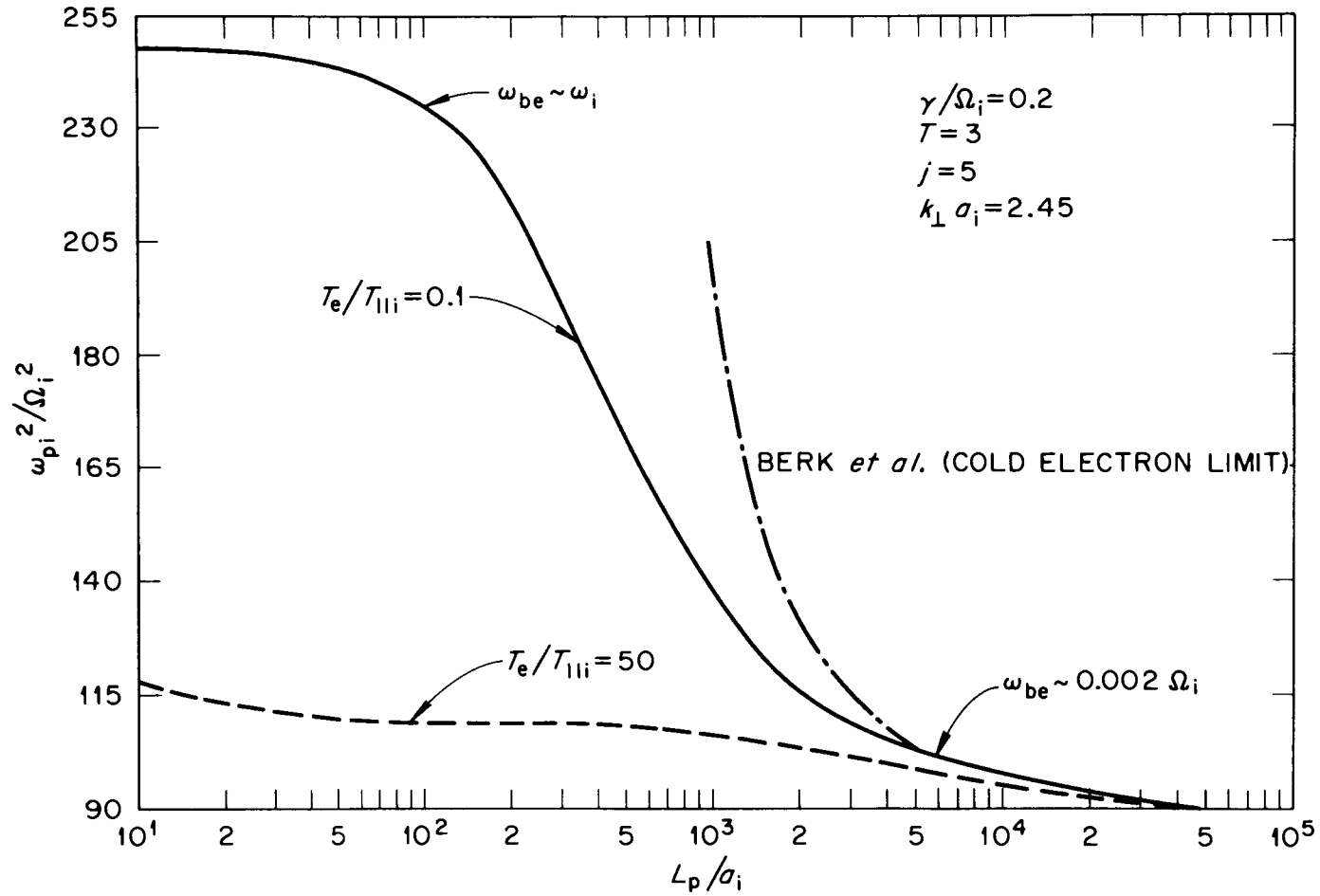


Fig. 10

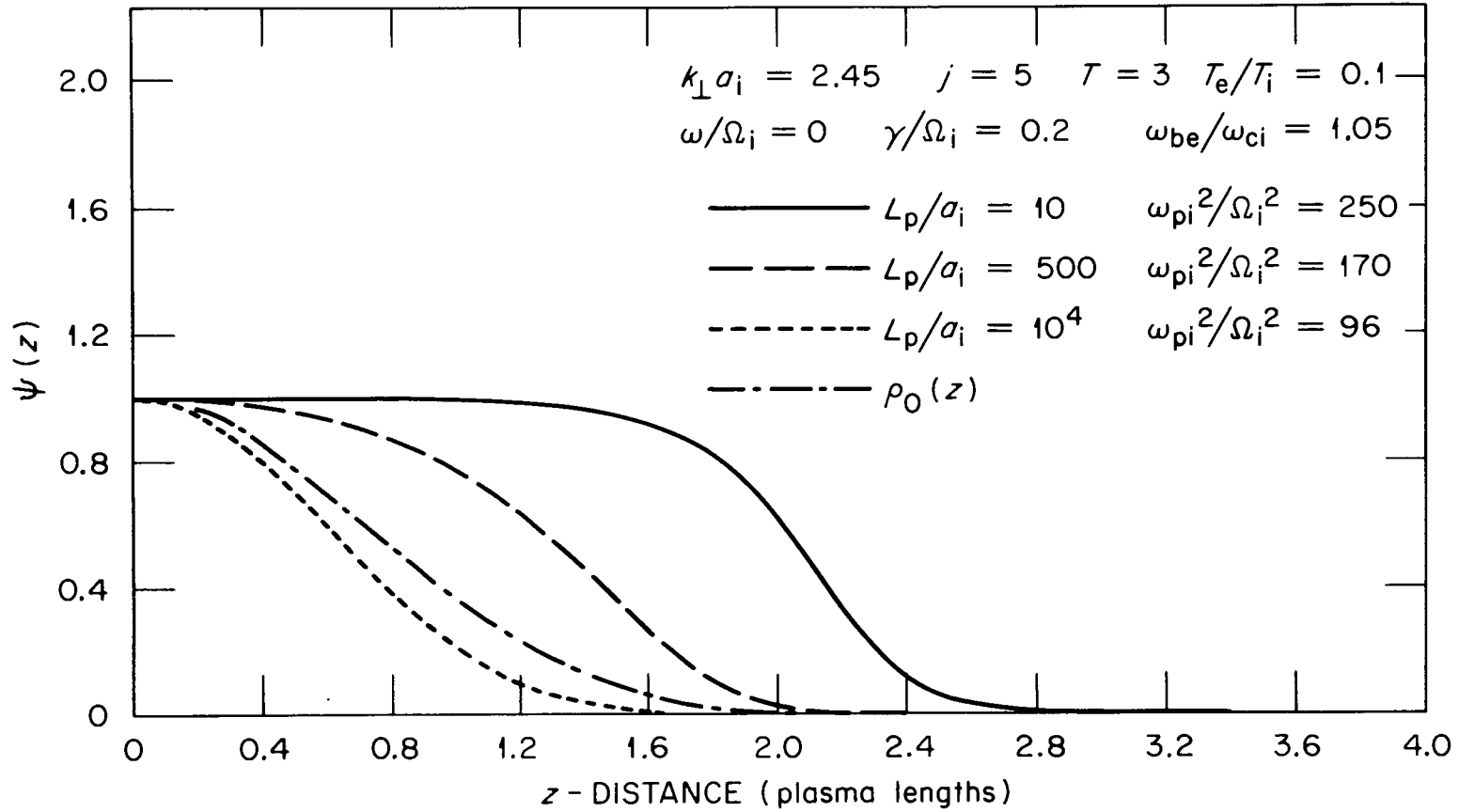


Fig. 11

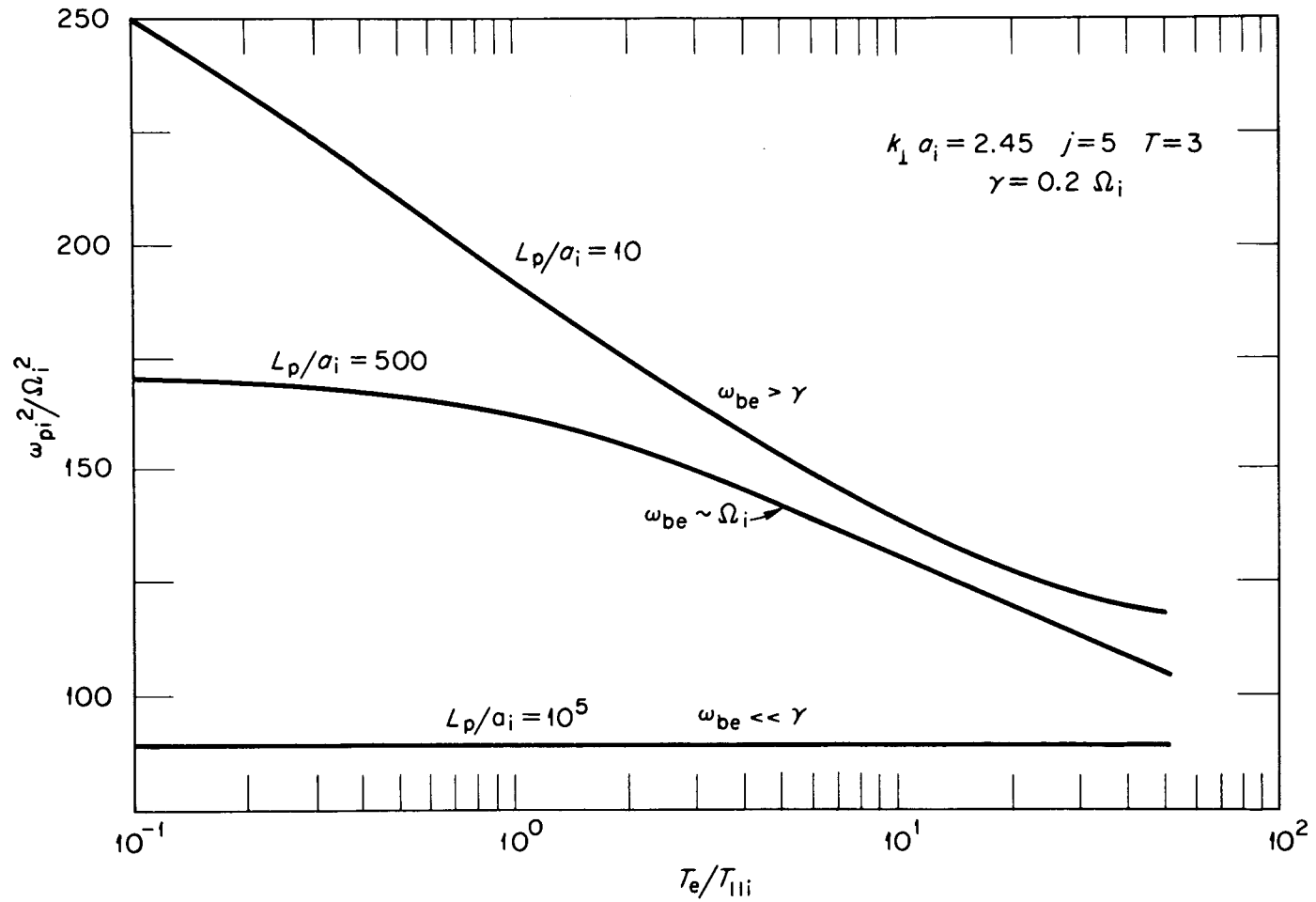


Fig. 12

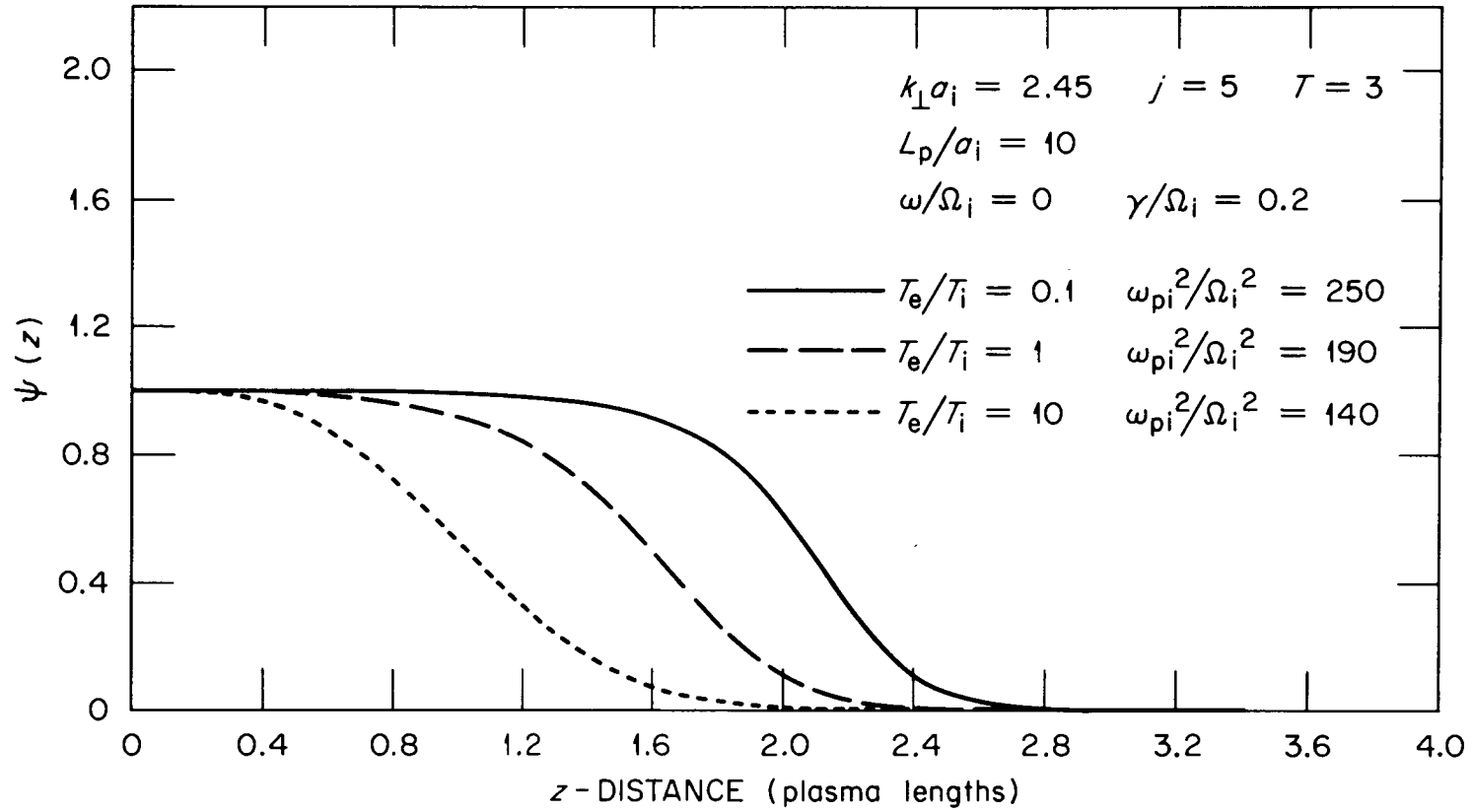


Fig. 13

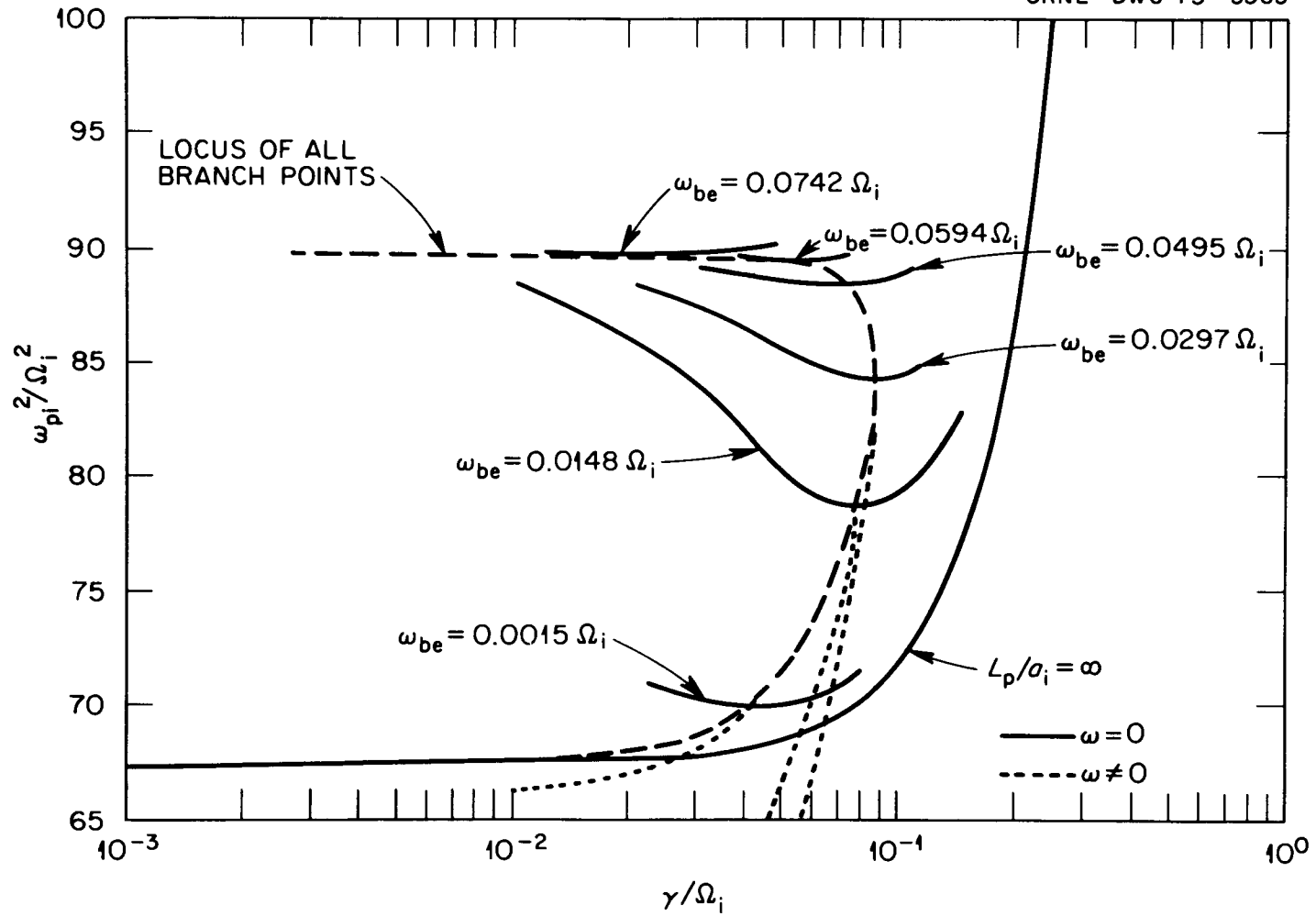


Fig. 14

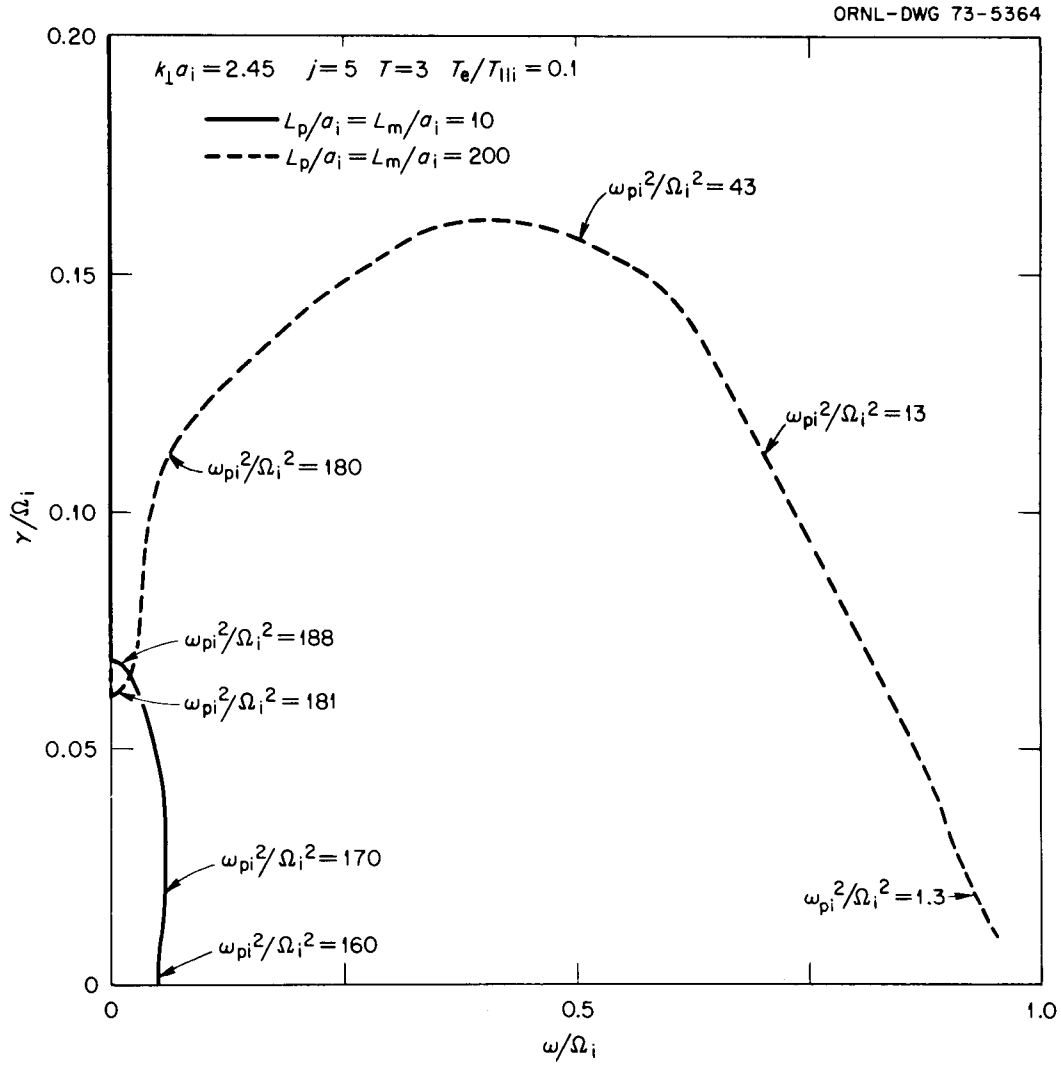


Fig. 15

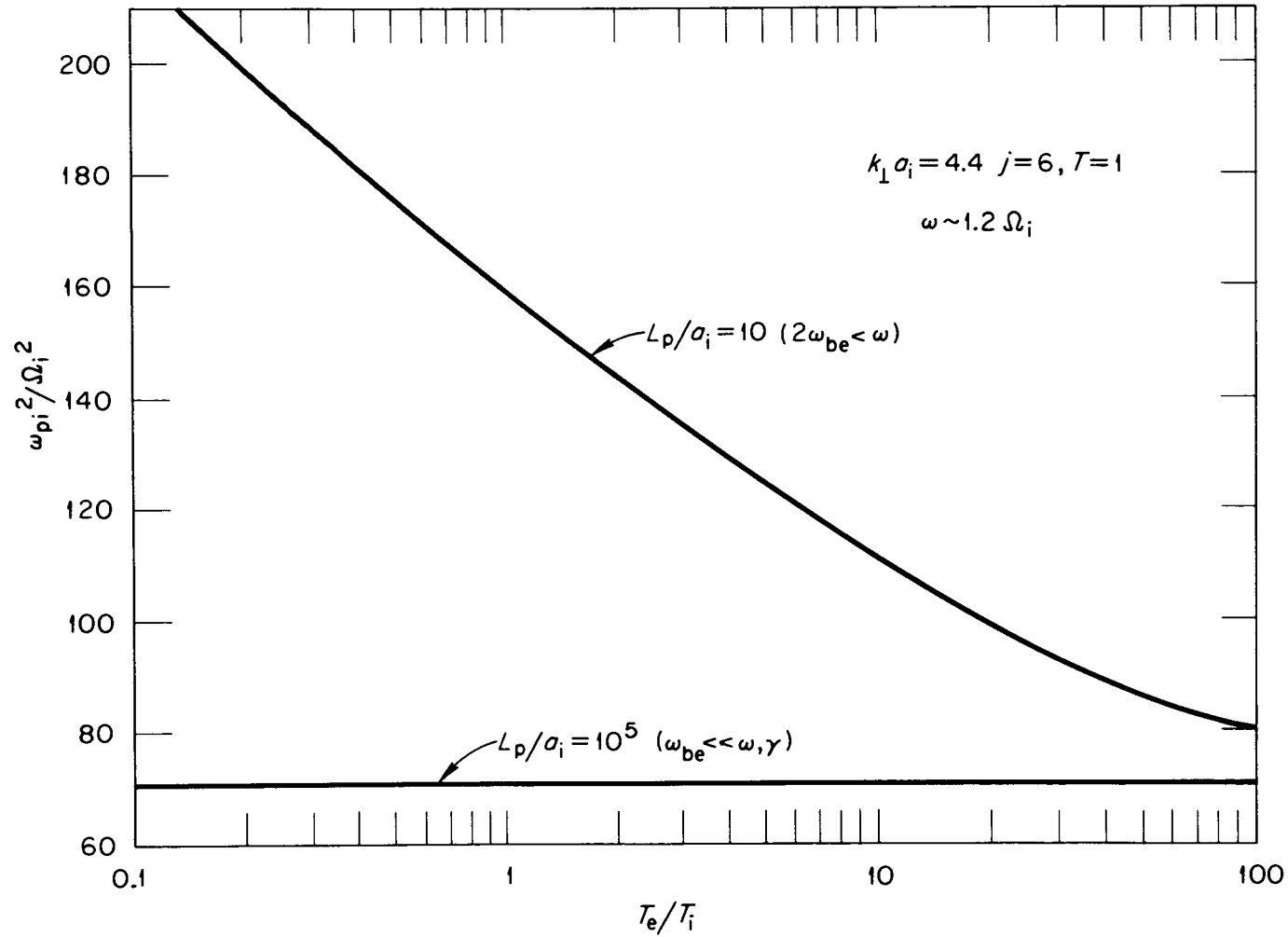


Fig. 16

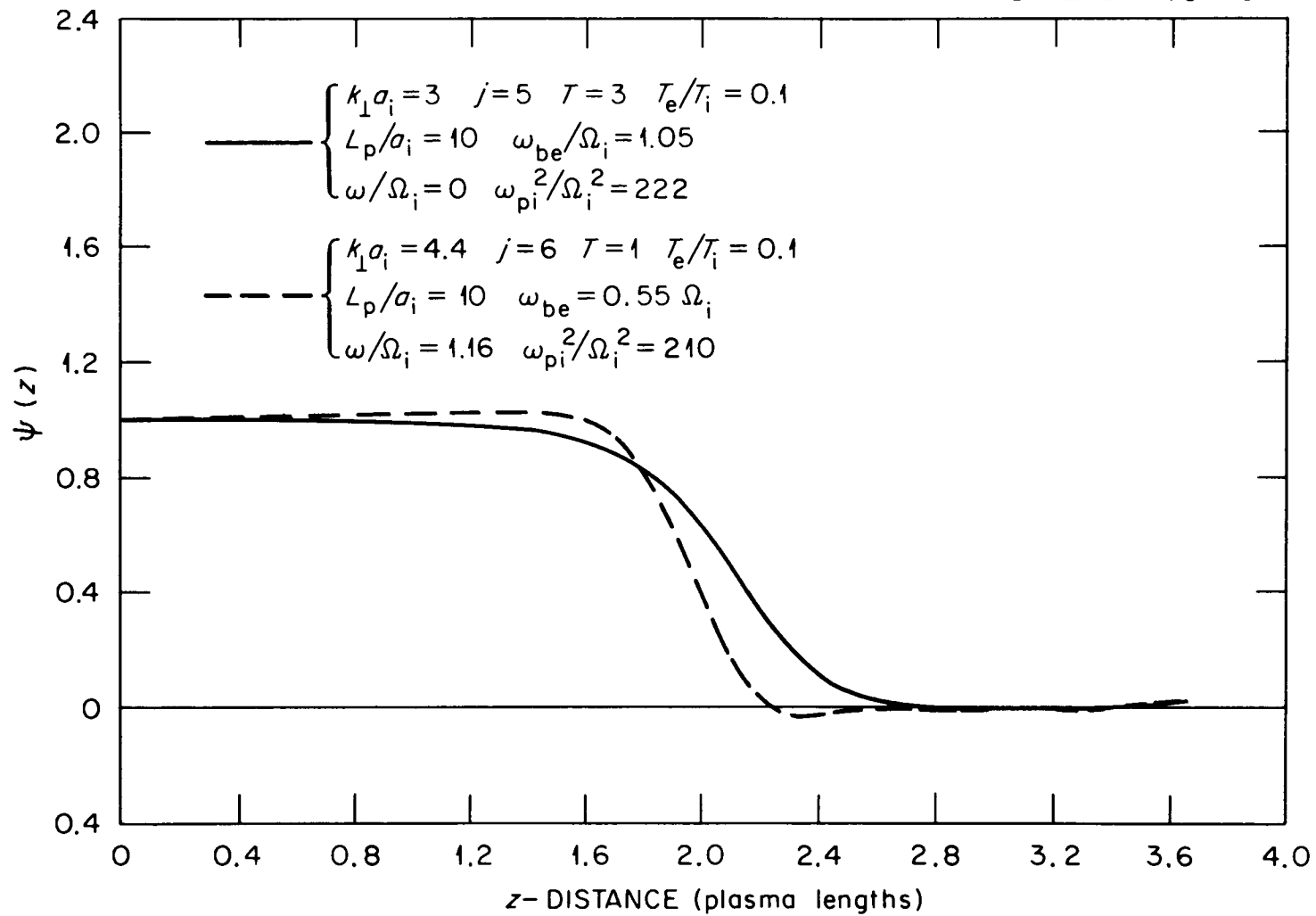


Fig. 17

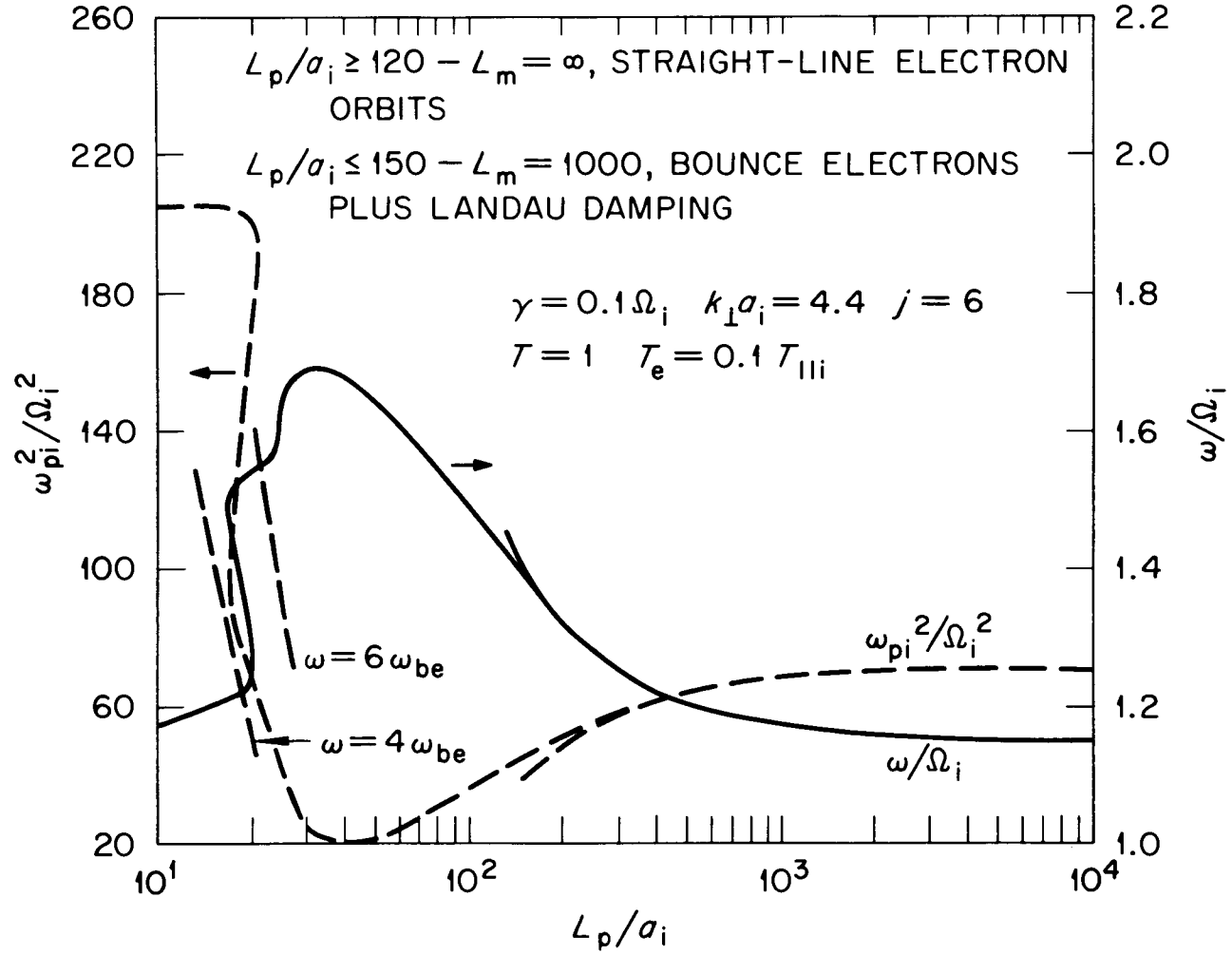


Fig. 18

ORNL-DWG 73-5360

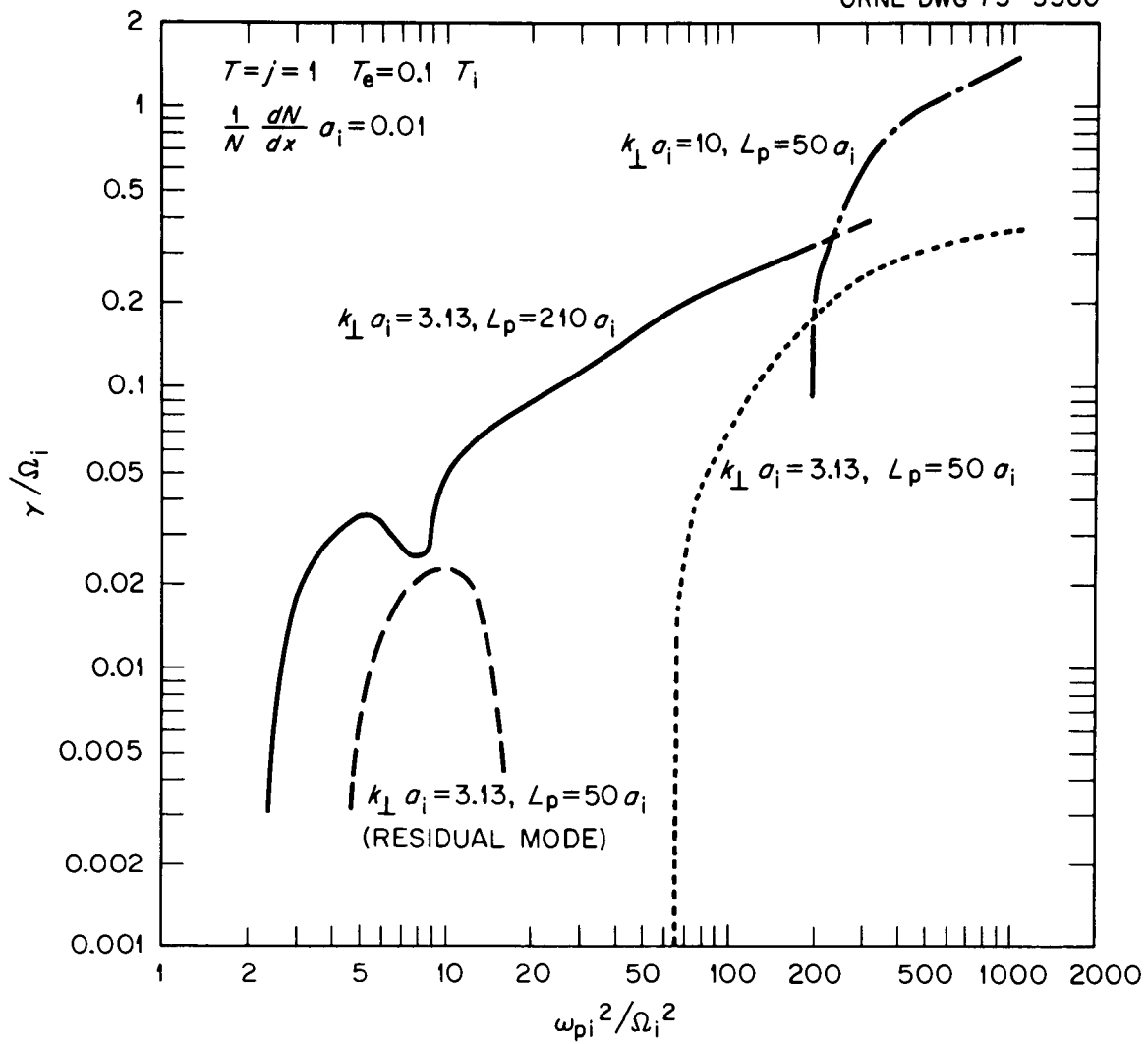


Fig. 19a

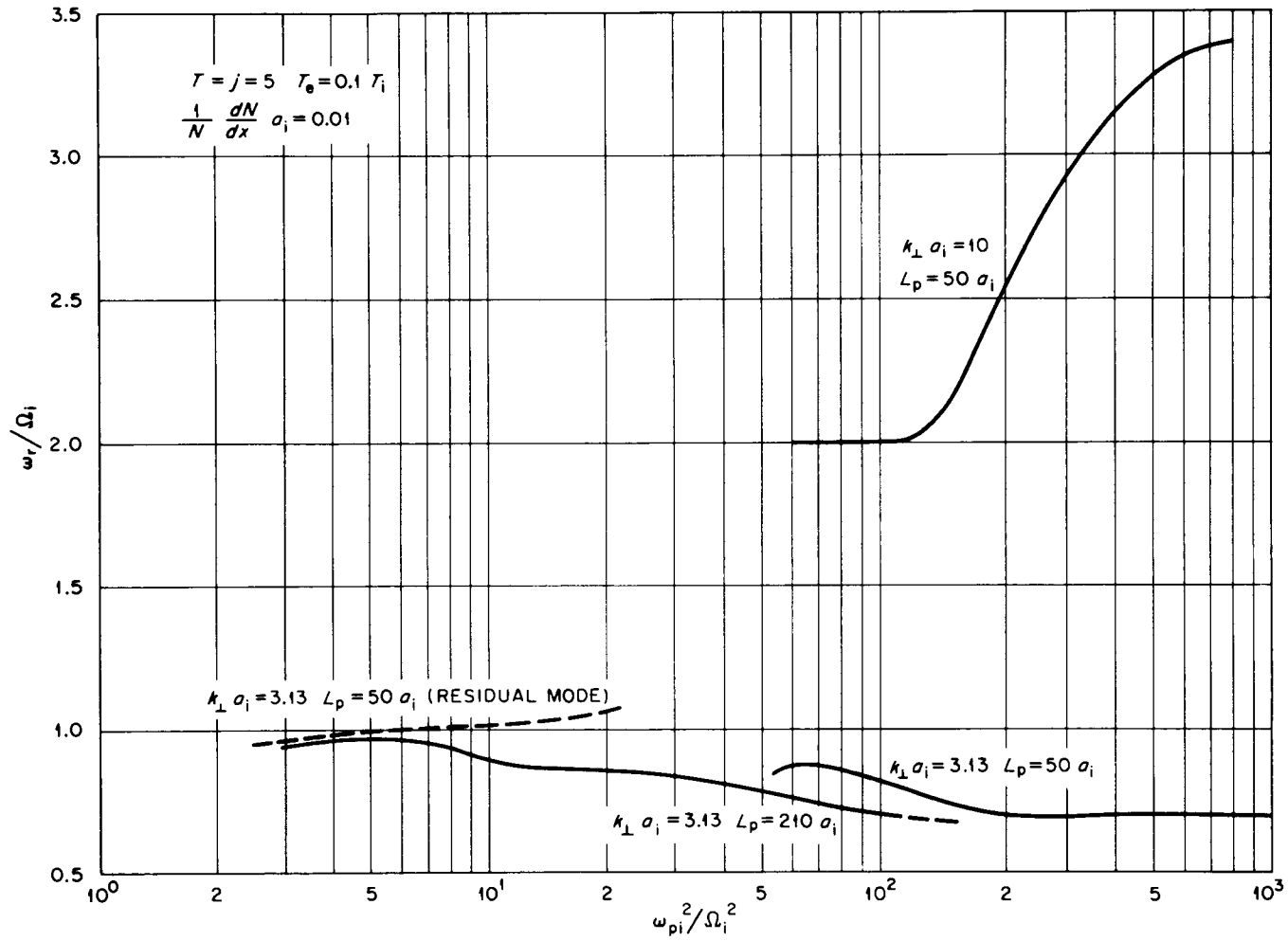


Fig. 19b

ORNL-DWG 73-7867

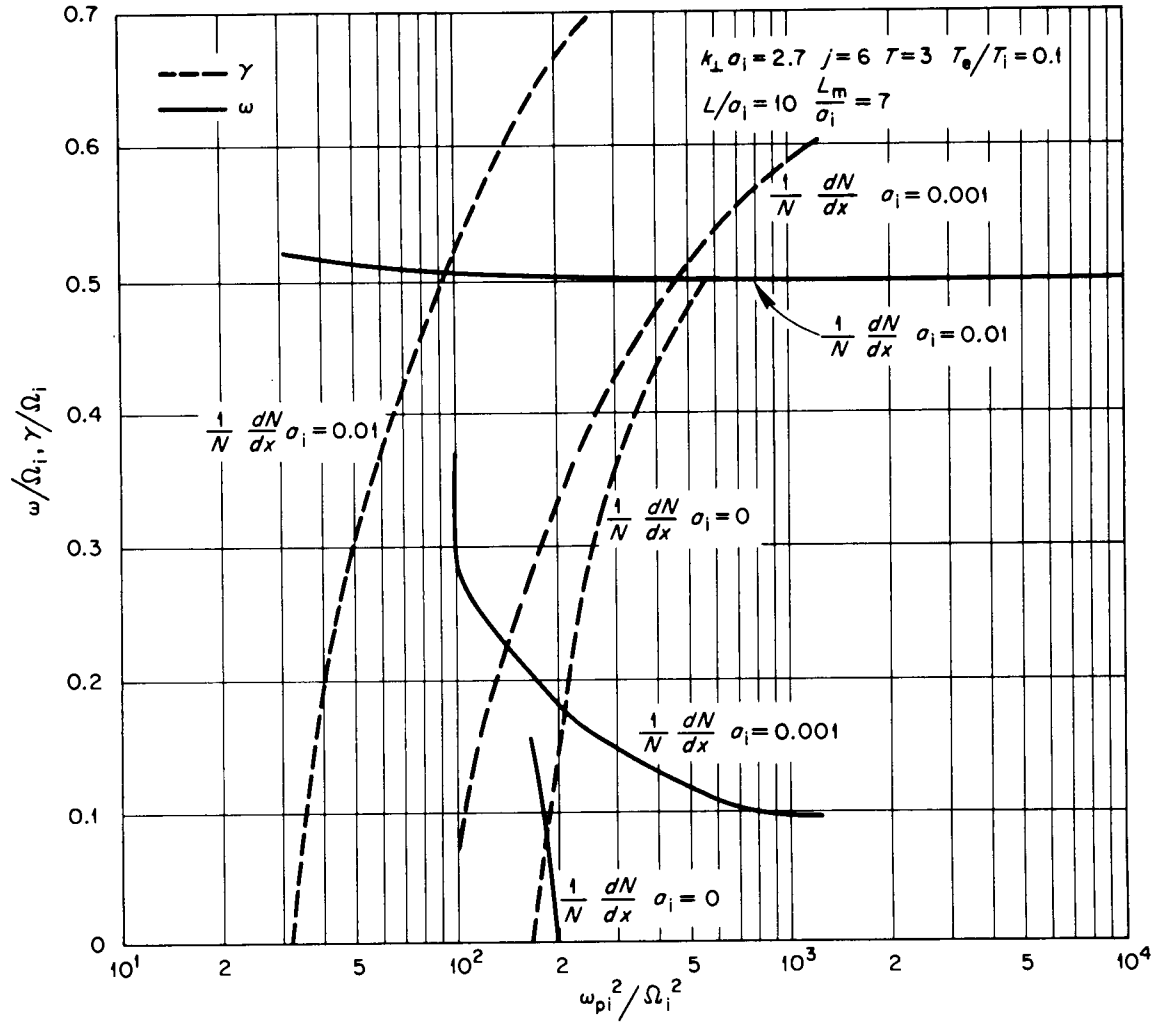


Fig. 20